Table Of Contents

I. FISCHER-TROPSCH SYNTHESIS ON IRON CATALYSTS

1. Background

1.1. Structure and Function of Active Phases in Fischer-Tropsch Synthesis

Fe-based oxides have been used as commercial catalysts for Fischer-Tropsch synthesis (FTS) to produce a wide range of paraffin and olefin products, ranging from methane to high molecular weight waxes [1]. During activation in synthesis gas and subsequent FTS reaction, several phases including metallic iron, iron carbides and iron oxides can co-exist at steady-state conditions [2-5]. The relative amounts of these phases depend on various activation and reaction conditions, which also lead to different catalytic performance. Some researchers [6] have proposed that surface iron atoms are responsible for FTS activity, while others have considered surface carbides or a mixture of carbides [7,8] with metallic iron [9] to be the active phase. There are also some reports that suggest that magnetite Fe_3O_4 is the active FTS phase [10-12]. Although these studies have each provided some evidence to support its specific proposal about the active phase, the available information remains phenomenological and sometimes contradictory, and a direct method to identify the active phase during reaction and to count the number of active sites has remained elusive. Based on our previous studies of the active phases and catalytic activity of Fe-Zn-K-Cu oxides [18-25], we have summarized in this reporting period with three manuscripts that address the structure and site requirement for Fe-based FTS catalysts.

1.2. Effects of Zn, Ru (Cu) and K on Fe Oxides

Many components have been incorporated into Fe catalysts in order to improve their mechanical and catalytic properties. Our previous studies have shown that Zn, K and Cu [13-15] promote the catalytic properties of Fe oxides. Zinc oxide, as a non-reducible oxide at FTS conditions, appears to stabilize the surface area of Fe oxide precursors. Alkali, as a modifier of the adsorption enthalpies of H_2 and CO, has been reported to increase the selectivity to desired C_{5+} products. Copper promotes the carburization processes and decreases the temperature required for the activation of iron oxide precursors. According to our previous optimum composition of Fe-Zn-K-Cu (Zn/Fe=0.1, K/Fe=0.02, Cu/Fe=0.01), we have prepared a series of Zn and Fe co-precipitated oxides with constant Zn/Fe and K/Fe atomic ratios (Zn/Fe=0.1, K/Fe=0.02) and varying amounts of Ru (Ru/Fe=0-0.01). Ru is a very active FTS catalyst. Ru was chosen in order to improve the catalytic activity and to minimize unfavorable water gas shift reactions, which can be catalyzed by the Cu component on Fe catalysts. Also, K was added in order to increase wax and alkene yields, while decreasing the production of undesirable methane products. The same effects of K are expected on Fe-Zn-Ru-K catalysts. The effect of K and Cu on the reduction/carburization and FTS reactions was discussed in detail in the manuscripts.

2. Synthesis Procedures

2.1 Higher Surface Area Fe-Zn-K-Cu Oxides

Fe-Zn-K-Cu catalysts were prepared by co-precipitation of iron and zinc nitrates following the procedure described in our previous report [18]. In order to produce high surface area samples, an alcohol (isopropanol or ethanol) was used instead of water in order to wash the precipitates before drying the precipitates. Isopropanol or ethanol was employed to reduce the pore mouth pinching caused by the surface tension of intrapore liquids during drying processes. Since the subsequent impregnation of an aqueous solution of $K_2(CO_3)$ and $Cu(NO_3)_2$ will introduce a substantial amount of water to the precursors, which becomes the major cause for decrease of surface areas during second dryings, we dissolved $K_2(CO_3)$ and $Cu(NO_3)_2$ using the least amount of water and diluted the solution using isopropanol or ethanol to the liquid volume needed for the incipient wetness impregnation. Then, the dried materials were treated in dry air at 543 K for 4 h. A larger amount of K (K/Fe=0.02-0.08) and Cu (Cu/Fe=0.02-0.04) were doped to the Fe-Zn oxide precursors in order to match their higher surface areas obtained by alcohol-wash.

2.2. Fe-Zn-Ru-K Oxides

The Fe-Zn-K-Ru catalysts used in this reporting period have been described in the previous quarterly report (25).

3. Catalyst Characterization

3.1. Protocols for the Characterization of Fe-based FTS Catalysts

This research program addresses the synthesis and the structural and catalytic characterization of active sites in Fe-based catalysts for FTS. We have designed a matrix of samples consisting of a systematic range of multicomponent catalysts in order to determine the number and type of surface sites present on fresh catalysts and on samples during and after FTS reaction (Table 1.1). Our objective is to develop rigorous relationships between the synthesis methods, the resulting catalyst structures, and their function in FTS reactions.

4. Structure and Site Requirement of Fe-Zn-K-Cu Oxides for Fischer-Tropsch Synthesis

The reduction, carburization, and catalytic properties of Fe-Zn-K-Cu oxides catalysts were examined using kinetic and spectroscopic methods at FTS conditions. The structure and site requirements for FTS reactions and the effect of K and Cu were discussed in the following manuscripts.

Table 1.1. Matrix of samples and characterization methods for FTS reaction

<table>
<tr><th colspan="3">Nominal Composition of the Catalysts</th><th rowspan="2">Characterization Before and After FTS</th><th rowspan="2">FTS reaction</th></tr>
<tr><th>Zn/Fe mole ratio</th><th>K/Fe (at.%)</th><th>Cu/Fe (at.%)</th></tr>
<tr><td rowspan="6">0</td><td rowspan="2">0</td><td>0</td><td rowspan="20">XRD

Surface area

In situ XAS

H_2-TPR

CO-TPR

Isotopic transient</td><td rowspan="20">Effect of reaction condition

220 °C
21.4 atm

235 °C
21.4 atm

270 °C
5 atm

Effect of CO_2 addition

Isotopic studies</td></tr>
<tr><td>1</td></tr>
<tr><td rowspan="3">2</td><td>0</td></tr>
<tr><td>1</td></tr>
<tr><td>2</td></tr>
<tr><td>4</td><td>1</td></tr>
<tr><td rowspan="2">0.05</td><td>0</td><td>0</td></tr>
<tr><td>2</td><td>1</td></tr>
<tr><td rowspan="10">0.1*</td><td rowspan="2">0</td><td>0</td></tr>
<tr><td>1</td></tr>
<tr><td rowspan="3">2</td><td>0</td></tr>
<tr><td>1</td></tr>
<tr><td>2</td></tr>
<tr><td rowspan="2">4*</td><td>1*</td></tr>
<tr><td>2*</td></tr>
<tr><td>6*</td><td>3*</td></tr>
<tr><td rowspan="2">8*</td><td>2*</td></tr>
<tr><td>4*</td></tr>
<tr><td rowspan="2">0.2</td><td>0</td><td>0</td></tr>
<tr><td>2</td><td>1</td></tr>
<tr><td rowspan="3">0.4</td><td>0</td><td>0</td></tr>
<tr><td>2</td><td>1</td></tr>
<tr><td>6</td><td>2</td></tr>
<tr><th>Zn/Fe</th><th>Ru/Fe (at.%)</th><th>K/Fe (at.%)</th></tr>
<tr><td rowspan="4">0.1</td><td>0.5</td><td rowspan="2">0</td></tr>
<tr><td>1</td></tr>
<tr><td>0.5</td><td rowspan="2">2</td></tr>
<tr><td>1</td></tr>
<tr><td rowspan="4">0.1*</td><td>0.5*</td><td rowspan="2">0*</td></tr>
<tr><td>1*</td></tr>
<tr><td>0.5*</td><td rowspan="2">2*</td></tr>
<tr><td>1*</td></tr>
</table>

* Samples treated by alcohol-wash.

4.1. Fischer-Tropsch synthesis catalysts based on Fe oxide precursors modified by Cu and K: structure and site requirements

Abstract

The reduction, carburization, and catalytic properties of Fischer-Tropsch synthesis (FTS) catalysts based on Fe-Cu were examined using kinetic and spectroscopic methods at reaction conditions. Fe_2O_3 precursors reduce to Fe_3O_4 and then carburize to form a mixture of $Fe_{2.5}C$ and Fe_3C in both CO and H_2/CO mixtures at 540-720 K. Oxygen removal initially occurs without FTS reaction as Fe_2O_3 forms inactive O-deficient Fe_2O_3 species during initial contact with synthesis gas at 523 K. FTS reactions start to occur as Fe_3O_4 forms and then rapidly converts to FeC_x. The onset of FTS activity requires only the conversion of surface layers to an active structure, which consists of FeC_x with steady-state surface coverages of oxygen and carbon vacancies formed in CO dissociation and O-removal steps during FTS. The gradual conversion of bulk Fe_3O_4 to FeC_x influences FTS rates and selectivity weakly, suggesting that the catalytic properties of these surface layers are largely independent of the presence of an oxide or carbide core. The presence of Cu and K increases the rate and the extent of Fe_3O_4 carburization during reaction and the Fischer-Tropsch synthesis rates, apparently by decreasing the size of the carbide crystallites formed during reaction.

1. INTRODUCTION

Fe, FeC_x, FeO_y can co-exist when Fe oxides are activated in reactive gases or used in Fischer-Tropsch synthesis (FTS) reactions [1]. The relative abundance of these phases depends on reaction conditions and it can influence catalytic properties. The presence and role of these phases remain controversial [2], because the detection of active sites is usually indirect and the results tend to provide infrequent snapshots of the catalyst structures as a function of time on stream, instead of a continuous record of structural transformations during FTS reactions. The present study addresses the characterization of the structure and stoichiometry of active phases formed from Fe oxide precursors during FTS using a combination of isothermal transient kinetic methods, *in situ* X-ray absorption spectroscopy, and steady-state FTS rate and selectivity measurements.

2. EXPERIMENTAL

Fe oxide precursors were prepared by precipitation of an aqueous solution of $Fe(NO_3)_3$ (Aldrich, 99.99%, 3.0 M) or a mixture of $Fe(NO_3)_3$ and $Zn(NO_3)_2$ (Aldrich, 99.99%, 1.4 M) with $(NH_4)_2CO_3$ (Aldrich, 99.9%, 1 M) at 353 K and at constant pH of 7.0. The precipitates were treated in dry air at 393 K for 12 h and then at 643 K for 4 h. X-ray diffraction measurements confirmed that the crystal structure of resulting Fe oxides was Fe_2O_3. Fe oxide powders were impregnated with an aqueous solution of $Cu(NO_3)_2$ (Aldrich, 99.99%, Cu/Fe=0.01) and/or K_2CO_3 (Aldrich, 99.99%, K/Fe=0.02) using incipient wetness methods. The dried material was treated in air at 673 K for 4 h. Detailed descriptions of these synthesis

procedures are reported elsewhere [3]. The Cu-promoted oxide hereafter is designated as Fe_2O_3-Cu, and after K addition, as Fe_2O_3-K-Cu.

A rapid switch transient method was used to determine the extent and rate of reduction and carburization of Fe oxide precursors and the rate of FTS reactions during the initial stages of the catalytic reaction. Samples (0.2g) were pretreated in He (100 cm^3/min) up to 573 K and then cooled to 523 K. A H_2/CO/Ar stream (40/20/40 %, 1 atm, Matheson, 99.99%) was then introduced and the concentrations of gas products in the effluent stream were monitored using on-line mass spectrometry. Here, CH_4 formation rate was used as a surrogate measure of hydrocarbon formation rates because it can be measured accurately and changes with time on stream in parallel with the formation rates of other hydrocarbons. A pre-reduced Fe_3O_4-Cu sample was prepared by treating Fe_2O_3-Cu (0.2g, Cu/Fe=0.01) in 20 % H_2/Ar (100 cm^3/min) while increasing the temperature to 533 K at 0.167 Ks^{-1}. The Fe_3O_4 sample was then cooled to 523 K in He (100 cm^3/min) before exposing it to the H_2/CO/Ar stream. A FeC_x-Cu sample ($Fe_{2.5}C$ and Fe_3C mixture) was also prepared by treating Fe_2O_3-Cu (0.2g, Cu/Fe=0.01) in 20 % CO/Ar (100 cm^3/min, Matheson, 99.99%) while heating to 673 K at 0.083 Ks^{-1}. The presence of Fe_3O_4 and FeC_x phases was confirmed by X-ray diffraction and by detailed oxygen removal and carbon introduction measurements [4].

X-ray absorption spectra were obtained at the Stanford Synchrotron Radiation Laboratory using a wiggler side-station (beamline 4-1). Fe K-edge X-ray absorption spectra were acquired during FTS in synthesis gas using an *in situ* X-ray absorption cell [5]. A precursor oxide sample (8 mg; diluted to 10 wt.% Fe with graphite) was placed within a thin quartz capillary. Synthesis gas (H_2/CO=2) was passed through the sample at 523 K and a space velocity of 30,000 h^{-1}. The spectra were recorded *in situ* as the structure of the catalysts developed with time on stream after exposure to synthesis gas (~14 h). In order to capture the phase evolution of the Fe oxide precursors during initial contact with synthesis gas, XAS spectra were also measured after rapidly cooling samples to room temperature while flowing He through the powder bed. The relative concentrations of Fe carbides and Fe oxides in the samples were obtained using principal component analysis and a linear combination of X-ray absorption near-edge spectra (XANES). The spectra of reference materials, Fe_2O_3, Fe_3O_4, and FeC_x, were fitted to the catalyst XANES in the region between 7.090 and 7.240 keV.

3. RESULTS AND DISCUSSION

Figure 1 shows the temperature-programmed reduction profile of Fe_2O_3-Cu in H_2 and its reduction/carburization in CO. The amount of oxygen removed as a function of temperature indicates that the reduction of Fe_2O_3-Cu in H_2 proceeds in two steps: Fe_2O_3 reduced to Fe_3O_4 (<600 K); then, Fe_3O_4 reduced to Fe at 600-950 K. The oxygen removal and carbon introduction rates as a function of temperature for the Fe_2O_3-Cu sample in CO suggest that reduction/carburization occurred also in two sequential steps, except that reduction started at ~80 K higher temperature in CO than in H_2. It appears that CuO reduced in H_2 at 470 K to form H_2 dissociation sites that increase Fe_2O_3 reduction rates. Carburization did not start until 550 K, as Fe_3O_4 started to reduce. The formation of Fe carbides occurred concurrently with

the reduction of Fe_3O_4. X-ray diffraction of samples treated in CO at 550 K and 750 K confirmed that reduction and carburization of Fe oxides in CO proceeds via two sequential steps: Fe_2O_3 reduces to Fe_3O_4, Fe_3O_4 reduces and carburizes to form a mixture of $Fe_{2.5}C$ and Fe_3C.

Mass spectrometric analysis of initial products formed on Fe_2O_3-Cu, Fe_3O_4-Cu and FeC_x-Cu after exposure to synthesis gas at 523 K was used in order to measure the rate of initial reduction and carburization of Fe oxides as well as the FTS rates. Figure 2 shows the oxygen removal by H_2 and CO forming H_2O and CO_2 and the CH_4 formation rates during the initial reduction/carburization in H_2/CO and during subsequent steady-state FTS on Fe_2O_3-Cu at 523 K. During the initial 60 s, oxygen was removed from Fe_2O_3-Cu; reduction occurred without the concurrent formation of CH_4 or other hydrocarbons. The oxygen removed under the first sharp peak arises from the reduction of CuO to Cu. The rest of the oxygen removed during the induction period corresponds to an average stoichiometry of $Fe_2O_{2.8}$. This indicates that O-deficient Fe_2O_3 is not active for FTS reaction. CH_4 formation rates started to increase after this induction period and reached steady-state values after removal of only about 1-2 equivalent layers of O-atoms (assuming that a monolayer consists of 10^{19} O-atom/m^2) in Fe_2O_3, suggesting the facile formation of active sites, which rapidly reached their steady-state site density.

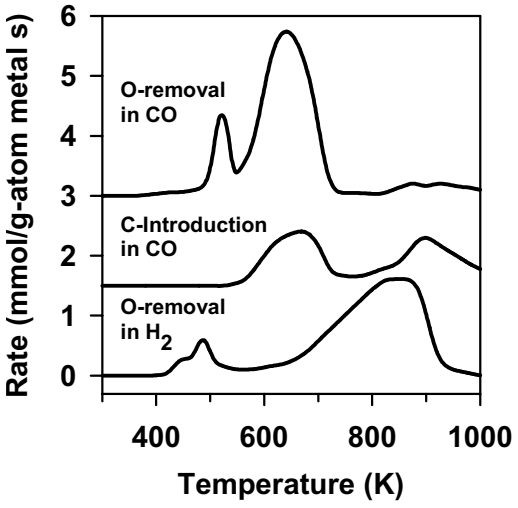

Fig. 1. Temperature-programmed reaction of Fe_2O_3-Cu in H_2 and CO (0.2 g sample; Cu/Fe=0.01, 0.167 Ks^{-1}; 20 % H_2 or CO in Ar; 100 cm^3/min total flow rate).

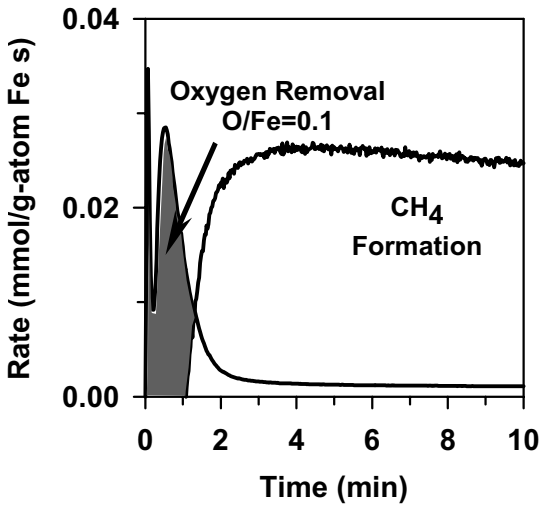

Fig. 2. Mass spectrometric product transients on Fe_2O_3-Cu with time on stream after exposure to synthesis gas at 523 K (0.2 g sample; Cu/Fe=0.01; H_2/CO=2, 100 cm^3/min total flow rate).

Figure 3 shows the results of linear combinations of Fe K-edge XANES for reference compounds (Fe_2O_3, Fe_3O_4 and FeC_x) as a description of the spectra measured for Fe_2O_3-Cu after exposure to synthesis gas at 523 K for various times. Fe_2O_3 rapidly disappeared during the induction period and Fe_3O_4 and Fe carbides formed concurrently; the extent of reduction and carburization increased with time on stream. Fe_3O_4 alone was never detected during FTS

reactions, indicating its facile conversion to Fe carbides. Fe metal was not detected at any time during exposure to synthesis gas at 523 K.

The structural changes from Fe_2O_3 to Fe_3O_4, the subsequent facile conversion of Fe_3O_4 to Fe carbides, and the concurrent increase in FTS rates suggest that FTS reactions first occur as Fe_3O_4 is formed and then rapidly converted to FeC_x. The extent of carburization continued to increase with time on stream, without a detectable increase in FTS reaction rates, indicating that only the incipient conversion of Fe_3O_4 to FeC_x was required for FTS reactions to occur at steady-state rates. In effect, only surface layers of Fe carbides appear to be required to form FTS active sites, irrespective of the structure and composition of the bulk phase. The catalytic properties of Fe carbides appear not to be influenced by a remaining Fe oxide core or by its ultimate conversion to FeC_x.

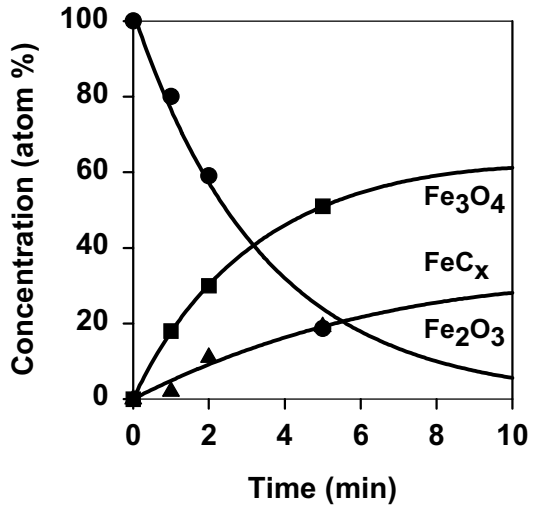

Fig. 3. Fe K-edge X-ray absorption measurements of the phase evolution of Fe_2O_3-Cu oxide with time on stream after exposure to synthesis gas at 523 K (1 mg, precipitated Fe_2O_3, Cu/Fe=0.01, H_2/CO=2, 30000 h^{-1}).

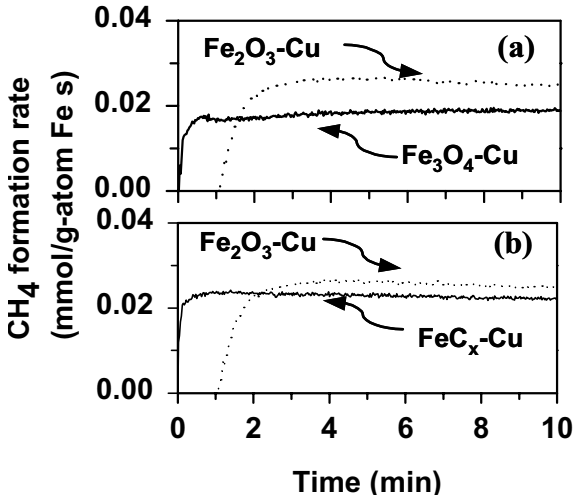

Fig. 4. Mass spectrometric product transients on (a) Fe_3O_4-Cu and (b) Fe_xC-Cu with time on stream after exposure to synthesis gas at 523 K (0.2 g sample; Cu/Fe=0.01; H_2/CO=2, 100 cm^3/min total flow rate).

Figure 4 shows the initial CH_4 transients on pre-carburized Fe carbides (FeC_x-Cu) and pre-reduced Fe oxides (Fe_3O_4-Cu) at 523 K during exposure to synthesis gas. Steady-state reaction rates were reached on both Fe_3O_4-Cu and FeC_x-Cu immediately upon contact with H_2/CO mixtures and without the induction period observed on Fe_2O_3 precursors. FTS rates remained constant even as the gradual removal of oxygen and the introduction of carbon continued to occur on Fe_3O_4-Cu. This indicates that the formation of an active surface occurred only after a few FTS turnovers, irrespective of the initial presence of Fe_3O_4 or FeC_x. This active surface is likely to consist of Fe carbides with a steady-state mixture of surface vacancies and adsorbed C and O atoms formed in the CO dissociation and O-removal steps required to complete a FTS catalytic turnover. The relative concentrations of these species are rapidly established by FTS elementary steps; they depend on the redox properties of the gas phase, on the reaction

temperature, and on the presence of any surface promoters that modify the redox properties of the surface.

Figure 5 shows steady-state hydrocarbon formation rates as a function of CO conversion on Fe_2O_3-Zn-Cu and Fe_2O_3-Zn-K-Cu (508 K, 21.4 bar, H_2/CO=2). ZnO species in these samples act as a structural promoter to increase FTS rates by inhibiting sintering of the oxide precursors during synthesis. The steady-state reaction data showed that the presence of Cu and K significantly increased FTS rates, suggesting that K and Cu increased the density of active sites formed during activation in H_2/CO mixtures.

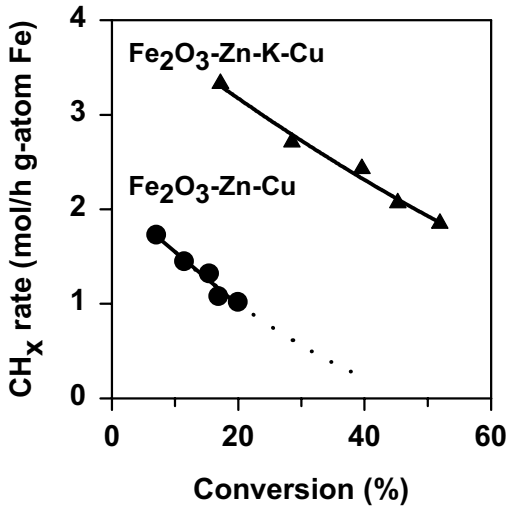

Fig. 5. Hydrocarbon formation rates as a function of CO conversion at steady-state FTS conditions (0.4 g sample; Zn/Fe=0.01, K/Fe=0.02, Cu/Fe=0.01, H_2/CO=2; 508 K, 21.4 atm).

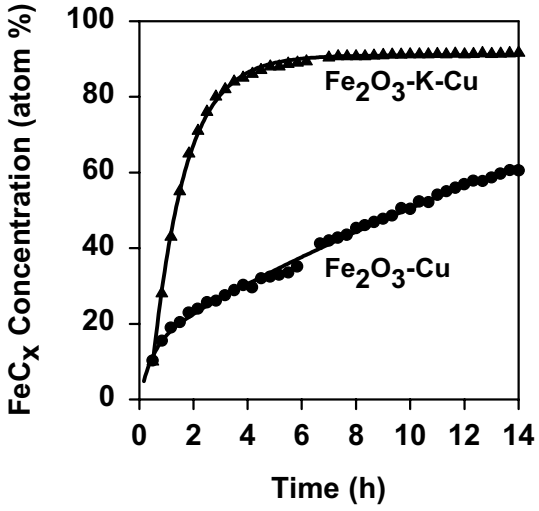

Fig. 6. *In situ* linear combination fits to Fe K-edge XANES of Fe_2O_3-K-Cu and Fe_2O_3-Cu as a function of time in synthesis gas at 523 K (1 mg sample; Cu/Fe=0.01, K/Fe=0.02; H_2/CO=2, 30000 h^{-1}).

The presence of Cu and of K increased the rate and the extent of Fe_3O_4 carburization during FTS reactions. The correlation between the rate and extent of carburization of these catalysts and their FTS rates appears to reflect the fact that K and Cu decrease the size of the carbide crystallites formed during reaction and thus increase the number of active sites. Our surface area and CO chemisorption measurements on the samples after FTS reactions confirmed that the surface areas and the amount of CO chemisorbed on the K- and Cu-containing samples are higher than on the samples without K and Cu. This supporting evidence will be described in a separate paper [6]. It appears that the smaller size of the crystallites formed in K- and Cu-containing samples account for their more complete carburization during FTS. It is not, however, their more complete carburization, but their higher surface area that accounts for higher FTS rates obtained on K and Cu promoted catalysts.

4. CONCLUSIONS

Porous Fe_2O_3 precursors sequentially reduce to Fe_3O_4 and then carburize to a mixture of Fe carbides ($Fe_{2.5}C$ and Fe_3C) in CO or in synthesis gas. The incipient conversion from Fe_3O_4 to Fe carbides occurs rapidly, at least in near surface layers, at FTS conditions. Oxygen removal initially occurs without FTS reaction as Fe_2O_3 forms inactive O-deficient Fe_2O_3 species during contact with synthesis gas. FTS reactions occur as Fe_3O_4 is formed and rapidly converted to FeC_x. FTS reactions require only the incipient conversion of surface layers to an active structure, which consists of FeC_x with a steady-state surface coverage of carbon and oxygen vacancies. The catalytic properties of Fe catalysts are not influenced by the gradual conversion of bulk Fe_3O_4 to FeC_x and its ultimate carburization at FTS conditions. The presence of Cu and of K increases the rates and extent of Fe_3O_4 carburization during reaction and the Fischer-Tropsch synthesis rates, apparently by providing multiple nucleation sites that lead to higher surface area FeC_x crystallites during reaction.

5. REFERENCES

1. R. B. Anderson, Catalysis; P. H. Emmett eds.; Van Nostrand-Reinhold: New York, Vol. 4, (1956) 29.
2. M. E. Dry, Catalysis-Science and Technology; J. R. Anderson, and M. Boudart eds.; Springer Verlag: New York, 1, (1981) 196.
3. S. L. Soled, E. Iglesia, S. Miseo, B. A. DeRites, R. A. Fiato, Topics in Catalysis, 2, (1995) 193.
4. S. Li, G. D. Meitzner, E. Iglesia, to be submitted to J. Catal.
5. D. G. Barton, Ph. D dissertation, University of California, Berkeley, 1998.
6. S. Li, G. D. Meitzner, E. Iglesia, to be submitted to J. Phys. Chem.

4.2. Structure and Site Evolution of Iron Oxide Catalyst Precursors during the Fischer-Tropsch Synthesis

Abstract

Reactions of Fe oxide precursors with synthesis gas lead to structural and chemical changes and to the formation of active sites for the Fischer-Tropsch synthesis (FTS). The local structure and oxidation state of Fe_2O_3 precursors promoted by Cu and/or K was probed using *in situ* X-ray absorption spectroscopy during these processes. The activation of these precursors occurs via reduction to Fe_3O_4 followed by carburization to form FeC_x. FTS reaction rates increase markedly during the initial stages of carburization, suggesting that the conversion of near-surface layers of Fe_3O_4 to FeC_x is sufficient for the formation of the required active sites. Thus, bulk structural probes, *ex situ* techniques without concurrent measurements of the products evolved during activation and FTS, can lead to misleading structure-function relations. The initial rate of carburization, and the extent of carburization and the FTS rate at steady-state, were higher for Fe_2O_3 precursors containing either Cu or K. These effects were stronger when both promoters were present. K and Cu provide CO and H_2 activation sites, which lead to the nucleation of multiple carbide regions on Fe oxide surfaces. The larger number of nucleation sites leads to higher initial carburization rates and to smaller FeC_x crystallites. These smaller crystallites, in turn, provide higher active surface areas, shorter bulk diffusion distances, more complete carburization of Fe_2O_3 precursors, and higher steady-state FTS rates. These effects of K and Cu on the number of available FeC_x sites were confirmed by titrating surface sites using CO after FTS reactions. It appears that K and Cu act predominantly as structural promoters, which increase the surface area of the active FeC_x phase. Chemical promotion of catalytic rates by these additives is not required in order to account for the observed results. These structural promotion effects of Cu and K account for the apparent correlation between bulk FeC_x contents and FTS rates at steady-state, even though the carburization of near-surface regions in bulk Fe_3O_4 appears to achieve steady-state FTS turnover rates.

Introduction

The Fischer-Tropsch synthesis (FTS) is an attractive route to clean transportation fuels and high molecular weight hydrocarbons from synthesis gas [1]. Fe-based catalysts are often used for this reaction because of their low cost, flexible product distribution, and ability to use coal-derived synthesis gas with low H2/CO ratios [2]. Ru and Co are also effective FTS catalysts [3,4]. Recently, Co-based catalysts have become the accepted compromise between cost and productivity for the synthesis clean diesel fuels. Fe-based catalysts complement this product slate by providing higher selectivity to olefins and oxygenates, which are useful as precursors to petrochemicals and to gasoline.

Several Fe phases, including α-Fe [5], Fe_3O_4 [6,7], θ-Fe_3C [8], ε'–$Fe_{2.2}C$ [9], χ–Fe_5C_2 [10], and Fe_7C_3 [11] have been detected in fresh and used Fe-based FTS catalysts. Most of these phases have been proposed at some point as the active species in FTS reactions. The relative abundance of these phases depends on reaction conditions. Even after many *ex situ* characterization studies, the composition of Fe-based FTS catalysts during reaction and the identity of the active phase remain controversial. Fe-based catalysts have been investigated by Mössbauer spectroscopy [10,12]; the time resolution of Mössbauer spectroscopy (>1 h for typical samples) precludes its use for *in situ* transient measurements during initial phase transformations. Also, Mössbauer spectroscopy is sensitive only to the recoil-free fraction, which depends on the structure of the Fe-containing phase. This recoil-free fraction must be accurately measured as a function of temperature for accurate structural assessments using Mössbauer spectroscopy. X-ray diffraction (XRD) cannot detect inorganic structures without long-range periodicity; as a result, it is not sensitive to amorphous or well-dispersed Fe species, which tend to account for a large fraction of the available surface area and of the active sites required for FTS. X-ray photoelectron spectroscopy (XPS) [7,13] has been used to examine catalytic solids before and after reaction, but it cannot be used during FTS. It requires quenching and catalyst cleansing procedures that influence the state of the surfaces probed by XPS. Recent high resolution transmission electron microscopy (HRTEM) studies have addressed the active phase of working Fe catalysts after different activation and reaction treatments; these studies have provided useful and novel insights about the nature of the working Fe catalysts [11,14]. However, none of these measurements were performed during reaction or even within the FT reactor. As a result, the relevant catalytic surfaces may have become restructured or contaminated, even with careful handling and controlled passivation.

X-ray absorption spectroscopy (XAS) can probe the local structure of inorganic structures, even as catalytic reactions occur, by using *in situ* spectroscopic cells with realistic and well-defined hydrodynamics. The X-ray absorption near-edge spectrum (XANES) is sensitive to the oxidation state and to the symmetry of the absorber atom [15]. Comparisons between these features and those in compounds with known local structure can be used to quantify the fraction of the absorbers present in each type of local coordination environment using principal component analysis (PCA) [16] and linear combination [17] methods. The region beyond the absorption edge contains oscillations in absorbance, which arise from the scattering of the emitted photoelectrons by atoms surrounding the absorber. This extended X-ray absorption fine structure (EXAFS) region of the spectrum contains information about the identity and the location of neighboring atoms coordinated to the absorber directly or through other atoms [15].

Therefore, X-ray absorption methods are ideally suited for *in situ* characterization of Fe-based FTS catalysts. We are not aware of its previous use for the structural characterization of Fe catalysts during FTS. Several reaction cells have been reported previously for *in situ* XAS measurements [18,19]. Here, we report a cell design based on modifications of one of these previously described cells [19] and use it to probe the local structure of Fe catalysts derived from Fe_2O_3 precursors during FTS. This study focuses on the evolution of the Fe_2O_3 component in the precursor materials during FTS reactions, and on the effect of various promoters (Cu, K), on the extent and the rate of the structural transformations that occur as Fe oxide catalyst precursors activate during contact with synthesis gas and as the FTS reaction approaches steady-state.

Experimental

X-Ray Absorption Sample Preparation

Fe K-edge X-ray absorption spectra were measured for reference compounds with known local structures and for catalyst precursors consisting of Fe-K-Cu oxides (K/Fe=0.02, Cu/Fe=0.01) during their reduction and carburization in CO and in synthesis gas. Fe_2O_3 (Alfa AESAR, 99.998%), Fe_3O_4 (Alfa AESAR, 99.997%), and FeO (Alfa AESAR, 99.5%) were used as reference materials. Fe_3C, which can form during FTS reactions, was prepared by temperature-programmed reaction (0.167 K/s) of Fe_2O_3 using CO (Matheson, 99.99%, 107 mol CO/g-atom Fe-h) as the reduction and carburization reagent at temperatures up to 973 K [20]. The resulting Fe_3C powder was passivated in flowing 1 % O_2/He (Matheson, 99.999%, 0.05 mol/h) at room temperature for 1 h before removing from the synthesis cell. X-ray diffraction measurements confirmed the exclusive presence of Fe_3C in this sample.

The Fe_2O_3 used for *in situ* XAS measurements was prepared by precipitation from an aqueous solution of $Fe(NO_3)_3$ (Aldrich, 99.99%, 3.0 M) with $(NH_4)_2CO_3$ (Aldrich, 99.9%, 1 M) at 353 K and a constant pH of 7.0. The precipitate was dried at 393 K overnight and treated in dry air at 643 K for 4 h. These oxide precursors were impregnated with aqueous solutions of K_2CO_3 (Aldrich, 99.99%,) and/or $Cu(NO_3)_2$ (Aldrich, 99.99%) to give K/Fe and Cu/Fe atomic ratios of 0.02 and 0.01, respectively. These compositions were found to give the best catalytic performance in the Fischer-Tropsch synthesis [21].

All samples used in spectroscopic measurements were diluted to 10 wt.% Fe with graphite powder (Alfa AESAR, 99.9995%, $S_g < 1$ m^2/g), pressed at 10 MPa, sieved to retain 180-250 μm particles, and placed within a quartz capillary cell [22]. The inertness of graphite was tested by flowing H_2 over Fe oxides mixed with graphite up to 873 K without any detectable formation of FeC_x. Also, no carbon oxide products were detected by mass spectrometry, indicating that neither FeO_x nor the Fe metal formed during reduction reacted with graphite at typical FTS temperatures (473-773 K). The maximum sample thickness was set by the inner diameter of the quartz capillary (0.8 mm). Reference compounds were also diluted with graphite to 10 wt.% Fe and held using a Prolene™ film against an Al plate containing a beam slit.

In Situ X-Ray Absorption Microreactor Cell

An *in situ* X-ray absorption reaction cell [22] was designed as a modified version of a previously reported reaction cell [19]. The modifications consisted of a finned heated block designed to replace the temperature control by heated air used in the earlier design. The cell consists of a quartz capillary (0.8 mm inner diameter, 0.1 mm wall thickness, 100 mm length) mounted horizontally into a stainless steel base using metal fittings and graphite ferrules (Figure 1). Samples with 180-250 μm particles form a dense bed through which gas flows with negligible pressure drop and plug-flow hydrodynamics. Heat is supplied by four cartridges heaters mounted into a finned copper block with a notch machined in order to contain the capillary tube and to provide a clear beam path. The copper block was insulated using a ceramic foam. A 20×4 mm beam path was cut into the finned copper block and the ceramic insulation in order to allow the X-ray beam (10×0.2 mm) to pass at a 45^{o} angle through the middle section of the capillary.

Gases were introduced into the cell from lecture bottles mounted in a portable gas manifold unit with built-in gas purifiers (O_2 remover; 13X molecular sieve; Matheson) and mass flow controllers (Porter Instruments). The desirable features of this XAS cell include small sample loadings (1-10 mg), low flow rates (1.3-13.4 mmol/h), and near plug-flow hydrodynamics, as well as the ability to attain conversions and space velocities similar to those typical of laboratory tubular microreactors. The capillary microreactor can reach temperatures of ~ 973 K and pressures up to 1.0 MPa. It also provides efficient heat transfer and accurate temperature control and measurement. A thermocouple (0.5 mm outer diameter) inserted into the outlet side of the capillary using a metal T-union provides accurate temperature measurement and prevents the sample from being dislodged from the capillary by the flowing gas. Temperature uniformity was confirmed by measuring the temperature profile along the sample bed under conditions identical to those used for the *in situ* experiments. The typical temperature variation along the sample bed is within ± 0.5 K. During *in situ* measurements, the cell temperatures can be controlled within ± 0.5 K in temperature-programmed or isothermal mode using a temperature controller (Series 982, Watlow). For the quench experiments described below, the capillary cell can be cooled to ambient temperature within a few seconds by merely sliding the heating block away from the capillary cell.

Measurements of X-ray Absorption Spectra

Fe K-edge X-ray absorption spectra were measured at the Stanford Synchrotron Radiation Laboratory (SSRL) on a wiggler side-station beamline (4-1). During these measurements, the storage ring was operated at 30-100 mA and 3.0 GeV. Two Si (111) crystals were used in the monochromator, which was detuned by 20% in order to eliminate harmonics from the monochromatic beam. Three N_2-filled ion chambers were used to measure the intensity of the X-ray beam incident on the sample (I_0), after the sample (I_1), and after a 5 μm Fe calibration foil (I_2). In this manner, the sample spectrum (I_0/I_1) and a reference spectrum (I_1/I_2) were obtained simultaneously. The most restrictive aperture along the beam path was the 0.2×12 mm slit within the hutch, which provided a resolution better than 2 eV at the Fe K-edge (7.112 keV) [23].

In order to achieve the required time resolution for spectrum measurements during temperature-programmed reduction and carburization in CO, a slow heating rate was used (0.017 K/s) and only near-edge spectra were measured (6.900-7.350 keV; 120 s per spectrum). After isothermal exposure to synthesis gas for 8-14 h, the spectra were recorded in the full energy range (6.900-

8.120 keV; 0.33 h per spectrum) in order to measure accurate spectra in both the near-edge and the fine structure regions.

X-Ray Absorption Data Analysis

X-ray absorption spectra were analyzed using WinXAS (version 1.2) [24]. Raw spectra were shifted in energy in order to align the first inflection point in the Fe foil calibration spectra with the known absorption energy of Fe metal (7.112 keV) [23]. Linear fits to the pre-edge region (6.900-7.100 keV) were subtracted from the spectra, and the spectra were normalized by a sixth-order polynomial fit of the post-edge region (7.240-8.120 keV). Principal component analysis [16] and linear combination methods [17] were used to calculate the relative abundance of the various Fe phases using the near-edge spectral region between 7.090 and 7.240 keV for each sample and for the Fe reference compounds.

The approach used to identify chemical species and to measure their relative abundance involves using linear combinations of the spectra from standard compounds, which include the structures thought to be present in the sample, to fit the measured near-edge spectra of samples. In the present case, it is difficult to anticipate which of the many possible Fe carbides, oxides, and oxycarbides may be formed during reactions with CO or with synthesis gas. Moreover, some species may be stable only under FT synthesis conditions. Thus, they are not necessarily available as structurally pure standards. In view of this, we have used principal component analysis (PCA) in order to identify sets of spectral features that increase or diminish in synchrony as the spectral series progresses. These sets of features comprise contributions from the spectra of chemical species that change in concentration as the sample evolves under *in situ* treatments.

During the reduction and carburization of Fe oxides in CO or in synthesis gas, PCA identified three major components involved in the phase changes; these components were Fe_2O_3, Fe_3O_4 and a carbide resembling Fe_3C. Therefore, *in situ* spectra were described using a linear combination of the near-edge spectra of these three standard compounds. Fe and FeO were specifically rejected by the PCA analysis, and their presence in linear combinations did not improve the spectral fits, suggesting that Fe and FeO do not occur as intermediates during reduction and carburization of Fe_2O_3 precursors. The target transform application of the PCA led to an excellent fit quality to Fe_3C, using components generated from our catalyst spectra. The analysis of the fine structure, however, indicated that the carburized Fe catalyst did not achieve sufficient long-range order to be rigorously described as a specific crystallographic phase of Fe carbide; therefore, we refer to it only as FeC_x throughout the rest of this report.

Fischer-Tropsch Synthesis Reaction Rate Measurements

Isothermal transient experiments to measure rates of product formation under FTS conditions, similar to those for *in situ* XAS measurements, were carried out using on-line mass spectrometric analysis. A 0.2 g sample diluted with graphite (0.5 g, 180-250 μm, Alfa AESAR, 99.998%) was loaded into a quartz microreactor and treated in He (Matheson, 99.999%, 0.268 mol/h) at temperatures up to 573 K and cooled under the same flow of He to 523 K. The He stream was switched to a flow of synthesis gas in Ar (H_2/CO/Ar=40/20/40 kPa, Matheson, 99.999%, total

flow rate 0.268 mol/h) at 523 K. The resulting isothermal transients in the rate of evolution of several FTS products (CH_4, H_2O and CO_2, etc.) were measured as a function of time using on-line mass spectrometry (Leybold Inficon, Transpector Series). The rate of formation of CH_4 was used as a surrogate measure of the total FTS rates, because it can be measured accurately and changes with time on stream in parallel with the rate of formation of other hydrocarbon products. At steady-state conditions, CH_4 selectivity changes with time on stream by less than 5%; therefore, CH_4 formation rates accurately reflect the total rate of hydrocarbon synthesis.

CO Chemisorption and Surface Area Measurements

Precipitated Fe oxides (0.2 g; diluted with graphite) were treated in flowing He (0.268 mol/h) up to 573 K and then cooled down to 523 K. The He stream was switched to a H_2/CO/Ar stream (40/20/40 kPa; 0.268 mol/h) at 523 K for 1 h and flushed with He (0.268 mol/h) at this temperature for 1 h in order to remove any reversibly adsorbed species. The samples were then cooled to room temperature (RT) before CO chemisorption and BET surface area measurements.

Two sets of temperature-programmed desorption (TPD) experiments were performed. In one experiment, a flow of CO/Ar stream (20/80 kPa; 0.268 mol/h) was passed through the sample for 0.5 h. Physisorbed species were removed by flushing the sample using Ar (0.268 mol/h) for 0.5 h. The amount of carbon species CO_x ($CO+CO_2$) evolved as the samples were heated in Ar flow (0.268 mol/h) at 0.167 K/s to 1000 K was measured by mass spectrometry. Another set of experiments followed the same protocol but without a CO chemisorption after FTS reaction. The difference between the peak areas under these two TPD curves was taken as a measure of the availability of active sites capable of chemisorbing CO reversibly at FTS temperatures. This method allows to subtract from the total CO evolved those CO species formed from irreversibly adsorbed carbon species during FTS, as well as the CO_x produced from reaction of FeC_x with remaining Fe oxides at temperatures much higher than that of FTS reactions.

BET surface area measurements were carried out after FTS reaction at 523 K and quenching to RT by passivating catalyst samples in flowing 1 % O_2/He at RT. N_2 physisorption measurements were performed at its boiling point (77 K) using an Autosorb 6 system (Quantachrome, Inc.). Surface areas were calculated using the BET method.

Results and Discussion

1. Fe K-edge XANES of Reference Compounds

Figure 2 shows the near-edge spectra for the Fe_3C, FeO, Fe_3O_4, and Fe_2O_3 reference compounds. The absorption edge at ~7.120 keV is caused by the ejection of Fe *1s* electrons after absorption of a photon. The measured absorption edge energies for all reference compounds are listed in Table 1. These binding energies of *1s* electrons increase with increasing Fe valence. The weak pre-edge features in the spectra of Fe oxides reflect electronic transitions from *1s* atomic orbitals to unoccupied *p-d* hybrid molecular orbital final states; these transitions are dipole-forbidden in non-centrosymmetric structures.

Table 1. Absorption edge energies for Fe compounds with known structure and oxidation state.

Compound	Fe	Fe_3C	FeO	Fe_3O_4	Fe_2O_3
Binding Energy (keV)	7.112	7.112	7.119	7.123	7.124

2. In Situ Fe K-edge XANES During Reactions of Fe Oxide Precursors with CO

Figure 3 shows Fe near-edge spectra for the Fe_2O_3 sample during exposure to CO. No detectable changes in the spectra occurred below 450 K. Gradual changes occurred at temperatures between 450 K and 600 K, but the spectra then remained unchanged at higher temperatures. Thus, it appears that the formation of a stable compound is complete by ~600 K. A qualitative comparison of the reference spectra (Figure 2) with those of the samples after exposure to CO (Figure 3) suggests that structural transformations involve the intermediate formation of Fe_3O_4 and its ultimate conversion to FeC_x.

A more quantitative assessment of these transformations is shown in Figure 4, which shows the relative abundances of the various phases required to describe the experimental near-edge spectra during reduction and carburization of Fe_2O_3 in CO. The reduction of Fe_2O_3 did not start until ~450 K. Above 450 K, the relative abundance of Fe_3O_4 increased, and then it decreased above 550 K, as Fe_3O_4 was converted to FeC_x. The concentration profiles for Fe_2O_3, Fe_3O_4, and FeC_x suggest that these transformations occurred in a sequential manner. The evidence of rapid conversion of Fe_3O_4 to FeC_x (Figure 4) was provided by detailed temperature-programmed reduction and carburization studies of Fe_2O_3 in CO [25] with concurrent measurements of the amounts of CO_2 evolved and of CO consumed. The reduction and carburization of Fe_2O_3 in synthesis gas (H_2/CO=2) followed the same reaction sequence as in CO, except that all structural changes occurred at slightly higher temperatures (~20 K).

3. In Situ X-Ray Absorption Spectra of Fe-Cu-K Oxide Precursors in Synthesis Gas

3.1. In Situ Fe K-edge XANES

Previous studies have shown that both K and Cu markedly increase FTS and water-gas shift rates [1,2]. K also increases the olefin content and the molecular weight of FTS products [26]. The evolution of the Fe near-edge spectral features in Fe and Fe-Cu-K oxide precursors during exposure to synthesis was used to examine the effects of H_2 in modifying the structural details detected during carburization in CO, as well as the role of the K and Cu on the rate and products of the transformation that occurs during the initial exposure of these oxide precursors to synthesis gas.

Figure 5 shows the near-edge spectra for Fe, Fe-Cu, Fe-K, and Fe-Cu-K oxide precursors measured *in situ* after contact with synthesis gas at 523 K for 5 h. The absorption edge energy was lower and the spectra resembled the Fe carbide spectrum (Figure 2) more closely when K or Cu was present in the sample. These effects of Cu or K were even stronger when both promoters were present.

3.2. Effects of K and Cu on Catalyst Structure and on Fischer-Tropsch Synthesis Rates

The spectra of Fe, Fe-Cu, Fe-K, and Fe-Cu-K oxide precursors during exposure to synthesis gas at 523 K were described by linear combinations of the near-edge spectra of reference compounds. The structural evolution of unpromoted Fe_2O_3 as a function of time is shown in Figure 6. The Fe_3O_4 and FeC_x contributions approached constant values of ~70% and ~30%, respectively, after ~ 4 h. Carburization rates then decreased as the remaining Fe oxides became covered by a dense Fe carbide coating, which appears to inhibit the rate-determining oxygen diffusion step in carburization processes. At 543 K, the FeC_x contribution increased to ~45% after 4 h, apparently because of the faster oxygen diffusion at these higher temperatures. Previous studies have suggested that the reduction and carburization (or nitridation) of transition-metal oxides is limited by the bulk diffusion of oxygen in the lattice of the corresponding oxide. This was inferred from the excellent agreement between the activation energies for the synthesis of transition-metal carbides or nitrides and those for the diffusion of oxygen in the oxides [27,28]. The absence of Fe metal or FeO in the near-edge spectra of these samples confirms the rate-determining nature of oxygen diffusion steps. If the removal of oxygen atoms at crystallite surfaces or at oxide-carbide interfaces had occurred without the immediate availability of carbon to react with the resulting reduced species, nucleation of Fe metal and FeO crystallites would have occurred.

Figure 7 shows the structural evolution of Fe-Cu oxide precursors (Cu/Fe = 0.01) during exposure to synthesis gas (H_2/CO=2) at 523 K for 14 h. These data show that Fe_2O_3 converts to Fe_3O_4, and subsequently to FeC_x more rapidly than for the pure Fe oxide samples (Figure 6). CuO reduces to Cu readily in H_2 at 523 K; once reduced, it provides sites for H_2 dissociation, which leads to adsorbed hydrogen species that reduce Fe_2O_3 to Fe_3O_4 at lower temperatures than for unpromoted Fe_2O_3.

The ultimate extent of carburization after long contact times (8 h) was also higher for Fe-Cu oxides (~45%; Figure 7) than for Fe oxide samples (~30%; Figure 6). The more complete carburization of Cu-containing Fe_2O_3 precursors would be unexpected without changes in the size of the crystalline structures, because carburization rates become ultimately controlled by the rate of oxygen diffusion. Oxygen diffusion rates cannot be influenced by the mere presence of Cu metal sites at the surface of such structures. Instead, it appears that the presence of Cu metal species at Fe_2O_3 surfaces leads to the simultaneous formation of a larger number of Fe_3O_4 or FeC_x nuclei, which then grow to consume a large fraction of the remaining Fe_2O_3 starting material. In contrast, the nucleation of these phases on pure Fe_2O_3 surfaces is likely to proceed through the formation of a uniform shrinking core of FeO_x encapsulated by a growing FeC_x layer. Our parallel XAS studies of the structural evolution of Fe_2O_3 during initial exposure to synthesis gas [25] have shown that Fe_2O_3, once reduced to Fe_3O_4, readily reduces and carburizes to FeC_x, at least for near-surface regions, as indicated by the concurrent formation of Fe_3O_4 and FeC_x and the rapid attainment of steady-state FTS reaction rates.

The conversion of Fe_3O_4 to Fe_3C is accompanied by a substantial decrease in crystallite volume, because of the lower density of the Fe_3O_4 (5.2 g/cm^3) compared with the FeC_x end product (7.7 g/cm^3 for Fe_3C) [29]. The dense Fe carbide layers formed at pure Fe_3O_4 surfaces apparently provide an effective barrier to the diffusion of oxygen. In addition, the carburization of the shrinking oxide core cannot continue to completion without the nucleation of a void or the

shattering of the carbide shell because of the density mismatch between the two phases. This shrinking core type of reduction agrees with the model proposed by previous studies of the reduction behaviors of transition-metal oxides [30].

The simultaneous formation of a larger number of FeC_x nuclei on Cu-promoted Fe_2O_3 leads to the selective growth of smaller carbide regions, which avoid both the longer diffusion paths and the void nucleation or shell breakup required for pure Fe_3O_4 surfaces. This leads, in turn, to more complete carburization and to smaller FeC_x particles, with a higher surface area and a smaller oxygen diffusion distance, and with a larger density of sites for CO activation**.** The apparent correlation between FTS rates and the extent of carburization is not causal. Instead, both reflect the smaller size of the active carbide structures that form during FTS when Cu is present on the Fe_2O_3 precursors. This finding resolves the puzzling effect of the extent of carburization on FTS rates, even when the formation of only a few near-surface layers of FeC_x leads to steady-state FTS reaction rates. Although only the incipient conversion of Fe_3O_4 to FeC_x is required for Fe_2O_3 or Cu-containing Fe_2O_3 precursors to become active in FTS reactions, the smaller and more extensively carburized formed when Cu is present lead to the higher FTS rates observed on Cu-containing Fe_2O_3 precursors [25]. As we describe immediately below, K has a similar effect as Cu on FTS rates and on the rate and extent of carburization of Fe_2O_3 precursors.

Fe_2O_3 precursors modified by K (K/Fe = 0.02) reduce and carburize even more rapidly than Cu-promoted Fe_2O_3 (Figure 8), consistent with our reduction and carburization kinetic measurements on these samples in both CO and H_2/CO reactants. The similar reduction-carburization promotion introduced by K in both CO and H_2/CO suggests that the role of K is to increase the rate of CO activation on Fe_2O_3 surfaces [25]. In contrast, the effect of Cu is most evident when H_2 is also present with CO, because of the role of Cu surfaces as H_2 dissociation sites. The presence of dispersed K species, probably as carbonate species, also leads to the rapid incipient formation of multiple Fe_3O_4 and FeC_x nuclei and to the ultimate formation of smaller crystallites with carbided surfaces. In this manner, we reconcile the similar directional effects of Cu and K on FTS reaction rates and the apparent contradiction between the positive effects of the higher extents of carburization induced by K and Cu and the increase in FTS reaction rates that appear to require only the near-surface conversion of Fe oxides to FeC_x [25]. During the incipient conversion of Fe oxides after exposure to synthesis gas, the CH_4 formation rate initially increased rapidly as a layer of FeC_x formed, and then it increased at a slower rate as the surface area of the FeC_x structures continued to increase gradually with increasing extent of carburization [25]. Ultimately both the FeC_x content and the FTS rates reached their steady-state values.

Reduction and carburization processes were even faster when both Cu and K were present (Figure 9) than when samples were promoted by either K or Cu (Figures 7 and 8). Apparently, the presence of a larger number of "activation sites" provided by the combined contributions of both Cu and K at Fe_2O_3 surfaces, leads to an even larger number of incipient nucleation points than when only one of these promoters is present. The resulting higher density of FeC_x nuclei ultimately grow into small crystallites, which provide a larger number of sites for CO and H_2 activation, leading to even faster reduction and carburization, shorter diffusion distances required for complete carburization, and faster FTS reaction rates than on singly-promoted samples.

The formation of smaller crystallites and of a higher density of active sites when K and/or Cu are present during activation is consistent with measurements of the BET surface area and the CO chemisorption capacity after FTS reactions for 1 h (H_2/CO=2, 523 K; Table 2). BET surface areas were higher on samples containing K and/or Cu, consistent with the formation of active catalysts containing smaller crystallites. CO chemisorption uptakes increased with increasing BET surface area. The site density available for CO chemisorption was higher on K- or Cu-containing samples. Chemisorption uptakes reached a maximum value on the Fe-K-Cu oxide precursor. These values correspond to about one monolayer (~15 CO/nm^2) of chemisorbed CO. This suggests that K and/or Cu promote the formation of smaller Fe carbide crystallites, which in turn increase the site density for CO adsorption/dissociation and consequently for the initial reduction and carburization and for steady-state FTS turnovers.

Table 2. The surface area and CO chemisorption results after 1 h FTS reactions; Fe carbide concentrations obtained from *in situ* XAS, and CH_4 formation rate from transient experiment, after 5 h FTS reactions.

Oxide precursor	Fe	Fe-Cu	Fe-K	Fe-K-Cu
Surface area (m^2/g)	13	17	18	23
Amount of CO_x desorbed before CO chemisorption (mmol/g-atom Fe)	12.2	14.1	23.4	56.9
Amount of CO_x desorbed after CO chemisorption (mmol/g-atom Fe)	20.3	27.9	40.9	95.7
Amount of CO chemisorbed (mmol/g-atom Fe)	8.1	13.8	17.5	38.8
CO chemisorption site density (molecule /nm^2)	5	6	7	13
FeC_x concentration[a] (atom %)	28.8	32.4	60.8	88.0
CH_4 formation rate[b] (mmol/g-atom Fe s)	0.061	0.070	0.11	0.19

[a]FeC_x concentration measured after exposure to synthesis gas at 523 K for 5 h (1 mg precipitated Fe_2O_3, K/Fe=0.02, Cu/Fe=0.01, H_2/CO=2, synthesis gas flow rate=107 mol/g-atom Fe h).
[b]CH_4 formation rates measured after exposure to synthesis gas at 523 K for 5 h (0.2 g precipitated Fe_2O_3, K/Fe=0.02, Cu/Fe=0.01, H_2/CO=2, synthesis gas flow rate=64.3 mol/g-atom Fe h).

In order to explore the relationships between the structure of the working catalysts and their catalytic performance, FTS rates were measured during exposure to synthesis gas at the same conditions (H_2/CO=2, 523 K) as the XAS experiments. Figure 10 shows the Fe carbide

concentrations obtained from *in situ* XAS and the CH_4 formation rates measured in transient experiments on unpromoted precipitated Fe_2O_3 as a function of time. The rate of formation of CH_4 increased with increasing FeC_x content. This indicates that Fe carbide (FeC_x) is the stable Fe phase during FTS and provides the active surfaces required for FTS turnovers. On samples containing K and/or Cu (Table 2), the FTS rates increase proportionally with the observed increase in FeC_x content (at long contact times) and in the CO chemisorption uptakes. This supports the conclusion that the effect of K and Cu on the structure of catalysts is to provide a larger number of active Fe carbide sites for FTS reactions. The chemical promotion effects by K and/or Cu do not appear to be necessary to account for the increase in reaction rates observed when Fe_2O_3 precursors are impregnated with these components. Cu does not influence the selectivity and the effects of K on FTS selectivity will be discussed in a subsequent paper [21].

Clearly, K and Cu lead to the formation of FeC_x structures with higher specific surface area and smaller size. A consequence of their smaller size is their more complete carburization, which is not the direct cause of the higher FTS rate observed in the presence of K and/or Cu. Their more complete carburization reflects the shorter diffusion paths for lattice oxygen species in the smaller crystallites, but the attainment of steady-state FTS rates appears to require only the formation of FeC_x near surface layers, the FTS activity of which do not depend on the existence or chemical identity of a separate oxide phase within the particle core.

Conclusions

Fe_2O_3 FTS catalyst precursors sequentially reduce to Fe_3O_4 and then carburize to FeC_x in CO or H_2/CO environments. The fast initial carburization of Fe_3O_4 becomes slower as diffusion of oxygen to the surface through a carbide shell. The nucleation of voids within the oxide particle core or the break-up of the carbide shell is required to accommodate the density mismatch between oxide and carbide phases. FTS rates increased proportionally with the extent of carburization and with the density of CO chemisorption sites in activated samples. This reflects the formation of smaller FeC_x structures when Cu or K lead to extensive nucleation of FeC_x structures during the activation of Fe_2O_3 precursors in CO or H_2/CO mixtures. The initial reduction and carburization rates of Fe oxides are promoted by Cu and K because of their role in rate-determining nucleation steps. The larger number of nuclei that ensue leads to more complete carburization and to a higher density of FTS active sites, present at the surface of FeC_x particles, which are likely to contain a residual, but catalytically irrelevant, Fe oxide core.

Acknowledgements

This work was supported by the U. S. Department of Energy (DOE) under contract number DE-FC26-98FT40308. X-ray absorption data were collected at the Stanford Synchrotron Radiation Laboratory (SSRL), which is operated by the Department of Energy (DOE), Office of Basic Energy Sciences under contract DE-ACO3-76SF00515.

Figure 1. X-ray absorption cell: (A) picture, (B) front view, (C) top view with the heating unit removed.

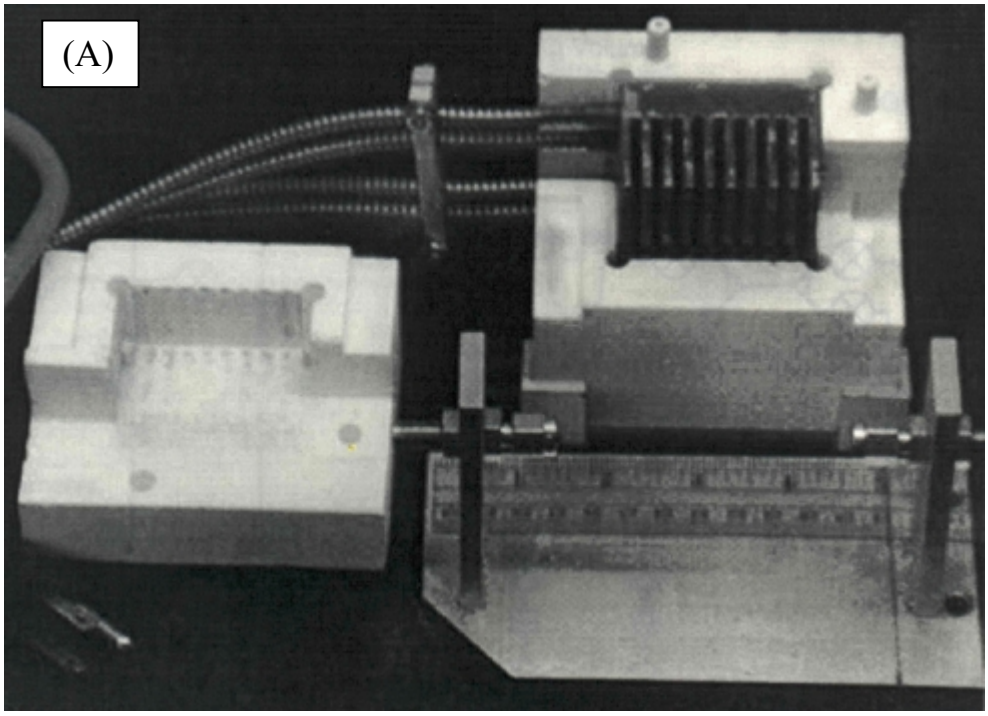

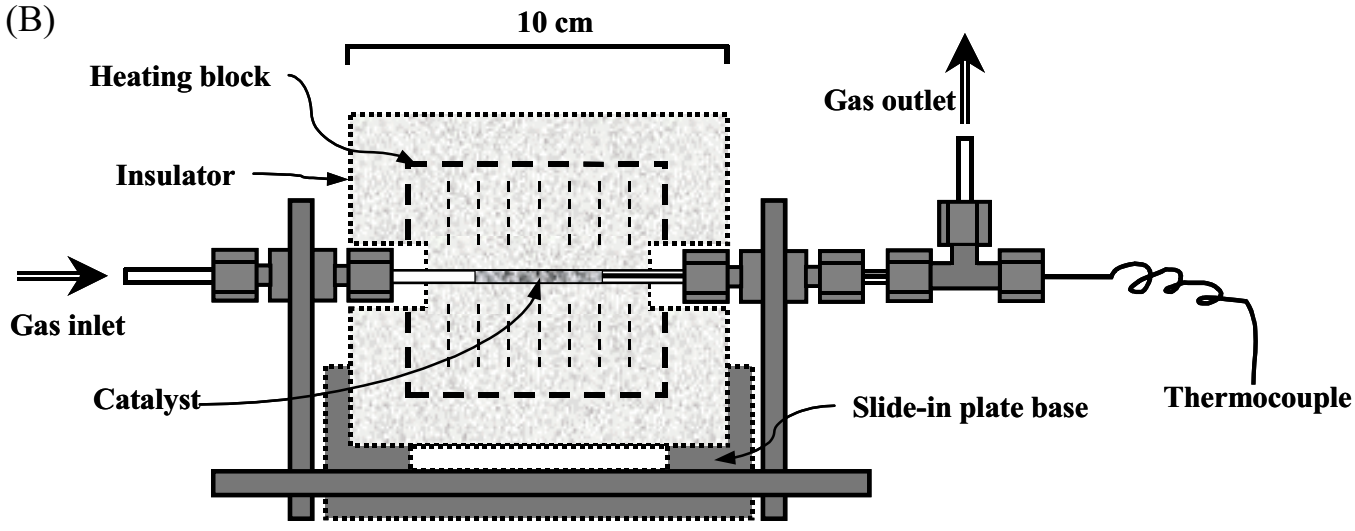

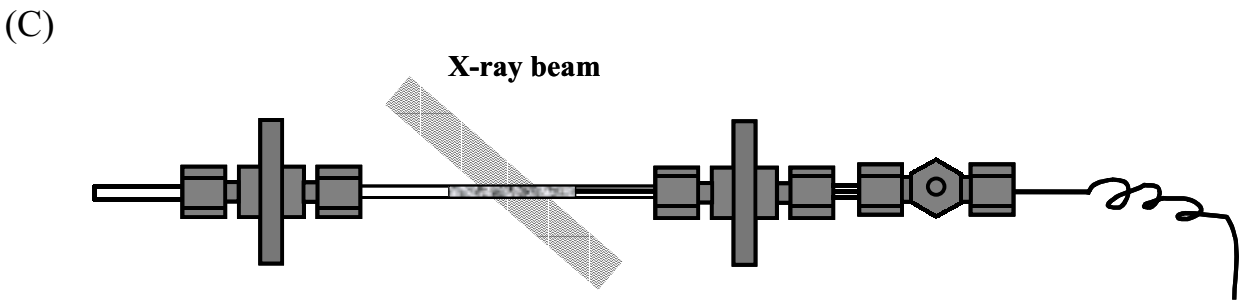

Figure 2. Normalized Fe K-edge X-ray absorption spectra for Fe oxides and carbide.

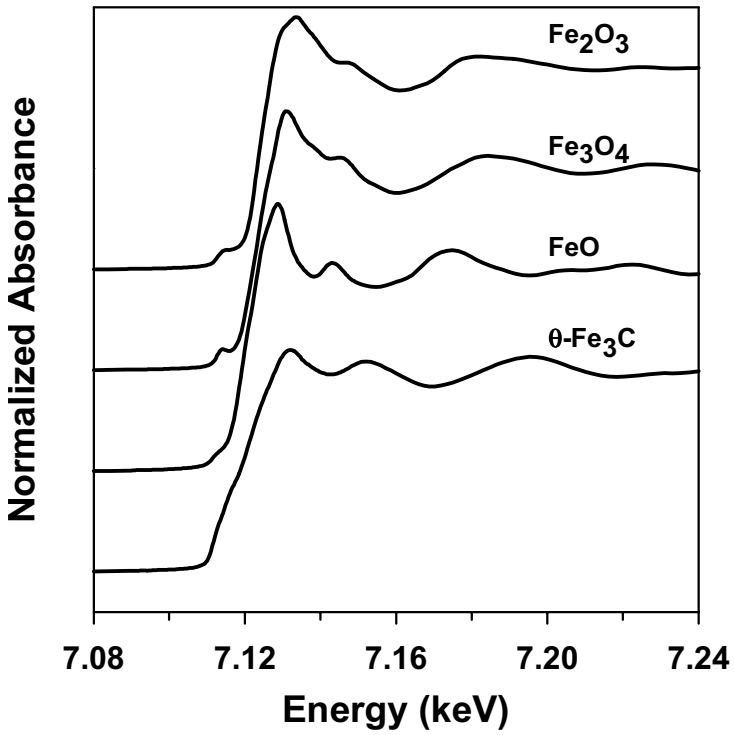

Figure 3. *In situ* Fe K-edge XANES spectra for Fe oxide in CO as a function of temperature. (1 mg precipitated Fe_2O_3, CO flow rate=107 mol/g-atom Fe h)

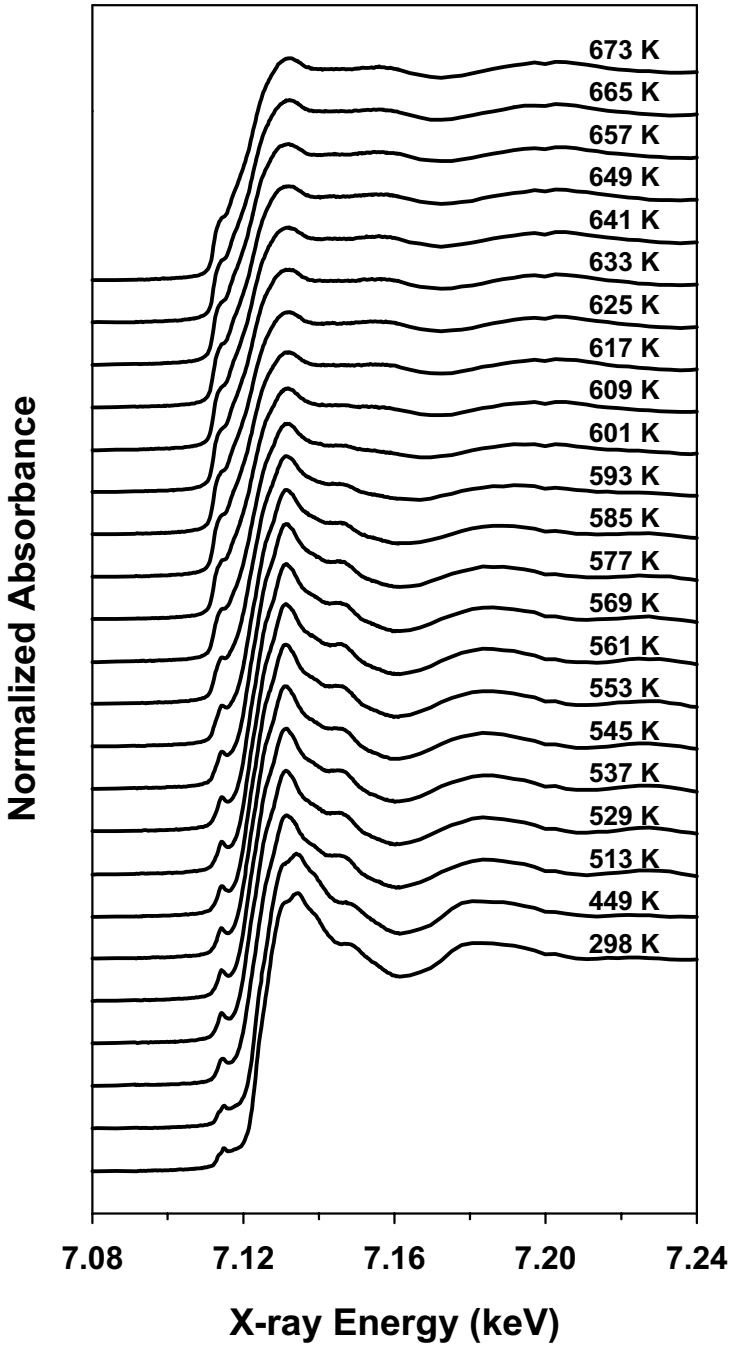

Figure 4. *In situ* evolution of Fe_2O_3 in CO as a function of temperature. Fe_2O_3 (dot), Fe_3O_4 (square), FeC_x (triangle). (1 mg precipitated Fe_2O_3, CO flow rate=107 mol/g-atom Fe h)

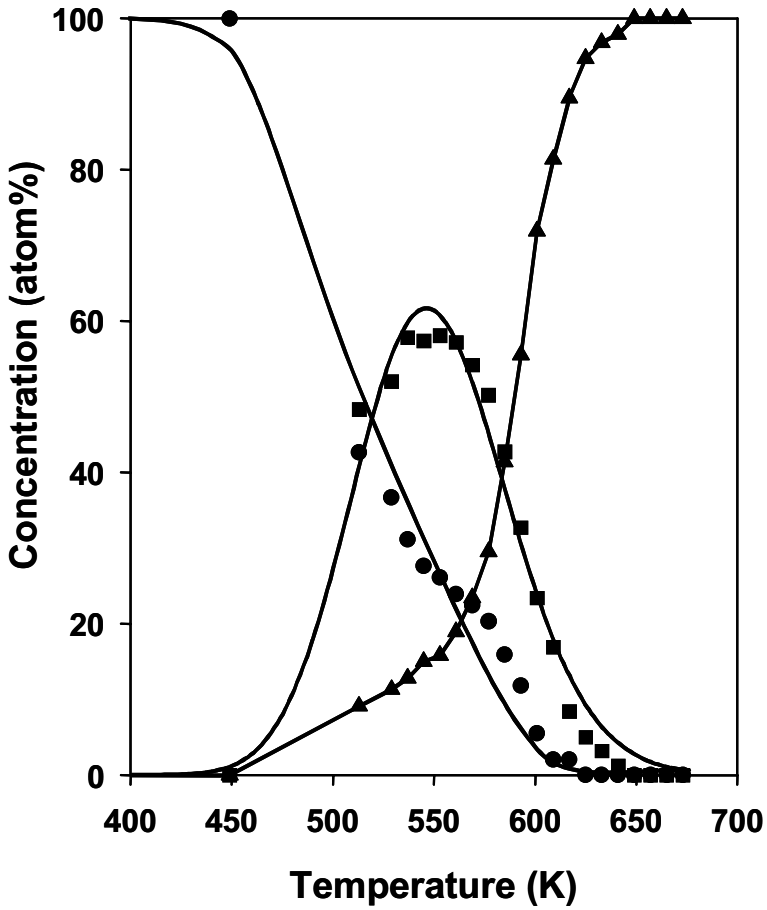

Figure 5. *In situ* Fe K-edge spectra of Fe-K-Cu oxides in synthesis gas at 523 K for 5 h. (1 mg precipitated Fe_2O_3, $H_2/CO=2$, synthesis gas flow rate=107 mol/g-atom Fe h).

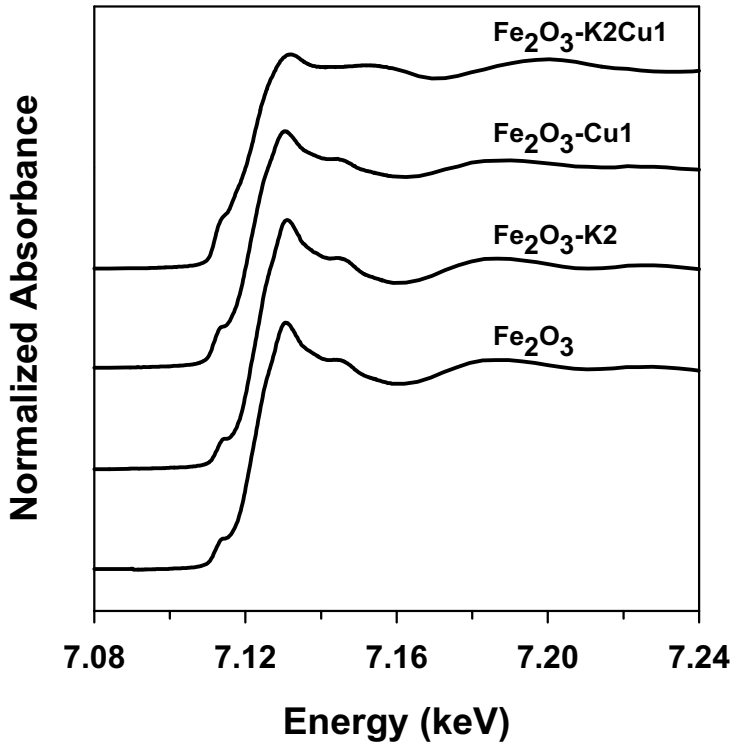

Figure 6. Phase evolution of Fe_2O_3 with time on stream after exposure to synthesis gas at 523 K (1 mg precipitated Fe_2O_3, $H_2/CO=2$, synthesis gas flow rate=107 mol/g-atom Fe h).

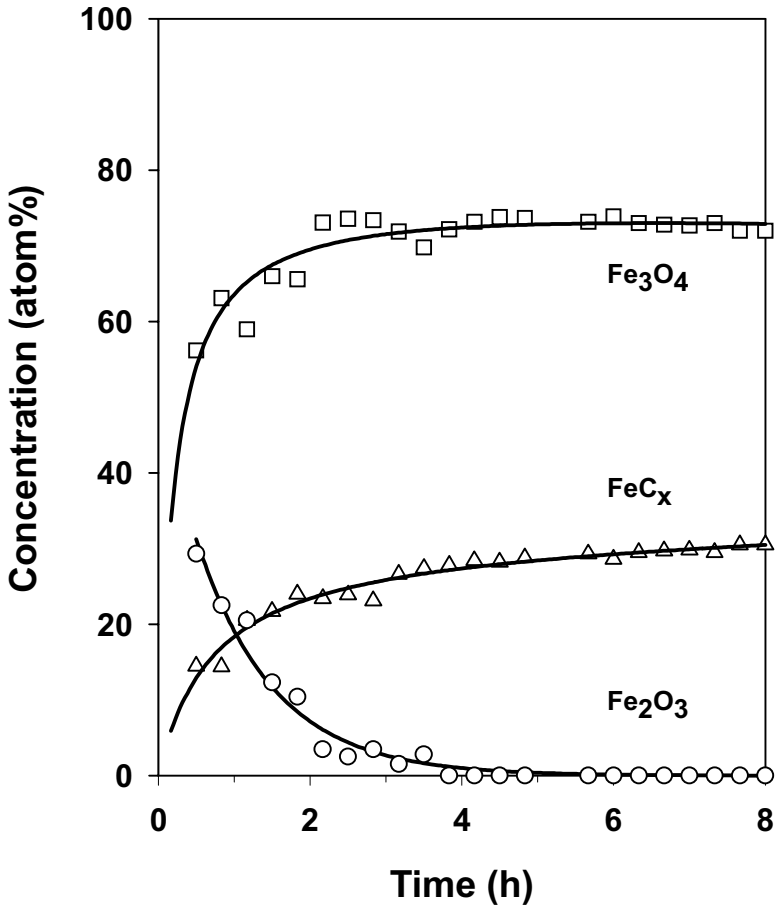

Figure 7. Phase evolution of Fe-Cu oxide with time on stream after exposure to synthesis gas at 523 K (1 mg precipitated Fe_2O_3, Cu/Fe=0.01, H_2/CO=2, synthesis gas flow rate=107 mol/g-atom Fe h).

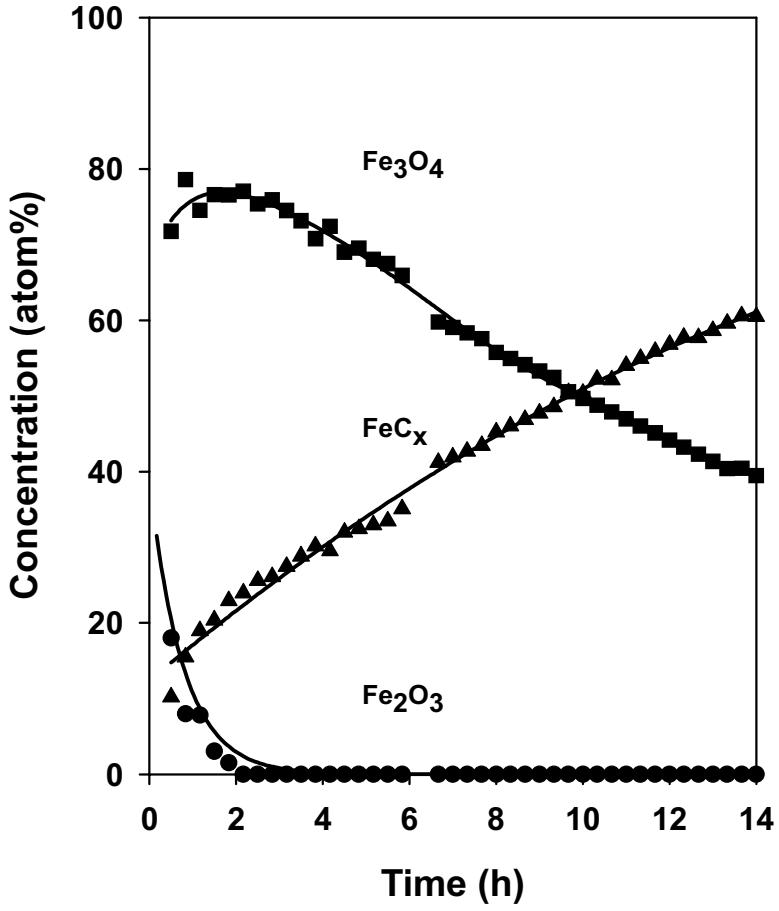

Figure 8. Phase evolution of Fe-K oxide with time on stream after exposure to synthesis gas at 523 K (1 mg precipitated Fe_2O_3, K/Fe=0.02, H_2/CO=2, synthesis gas flow rate=107 mol/g-atom Fe h).

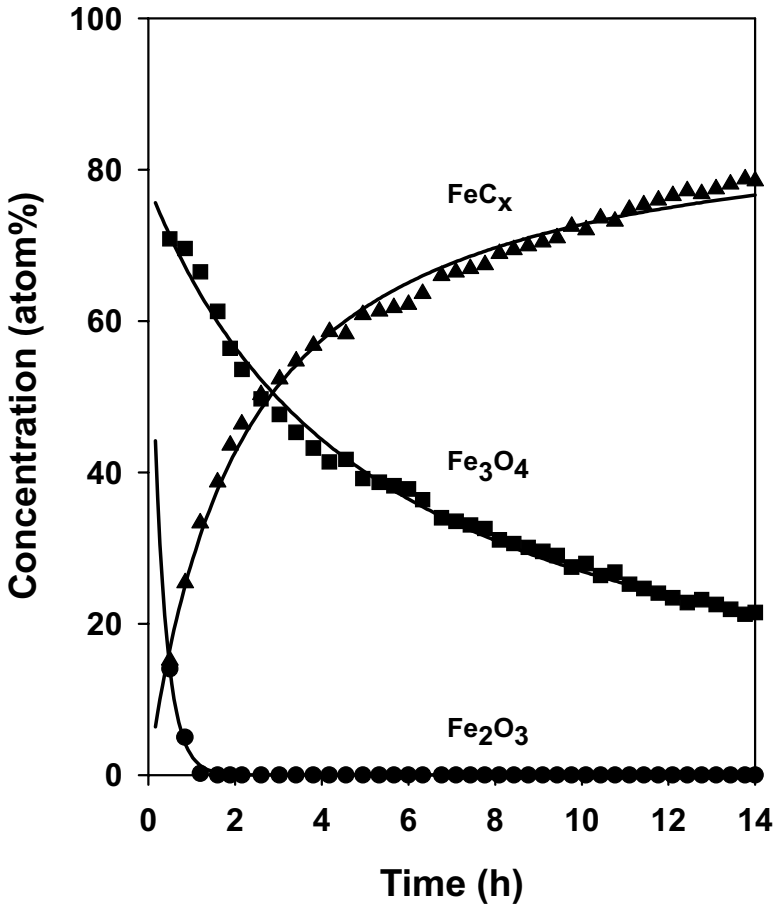

Figure 9. Phase evolution of Fe-K-Cu oxide with time on stream after exposure to synthesis gas at 523 K (1 mg precipitated Fe_2O_3, K/Fe=0.02, Cu/Fe=0.01, H_2/CO=2, synthesis gas flow rate=107 mol/g-atom Fe h).

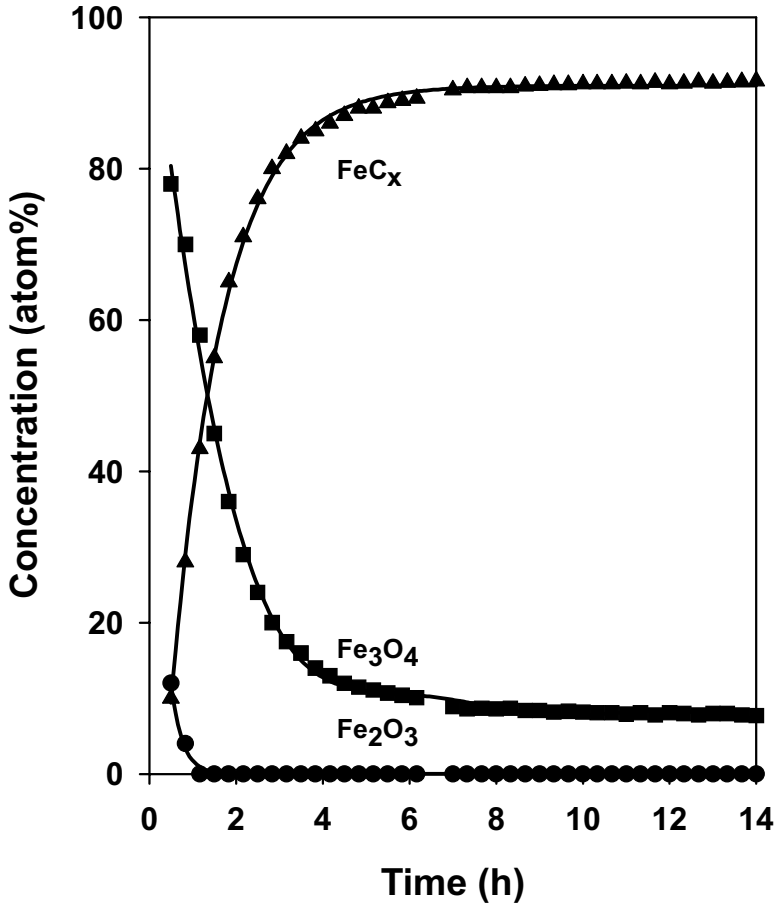

Figure 10. Fe carbide concentration (dots) obtained from XAS ($H_2/CO=2$, 523 K, synthesis gas flow rate=107 mol/g-atom Fe h), and CH_4 formation rate as function of time on unpromoted precipitated Fe_2O_3 ($H_2/CO=2$, 523 K, synthesis gas flow rate=64.3 mol/g-atom Fe h).

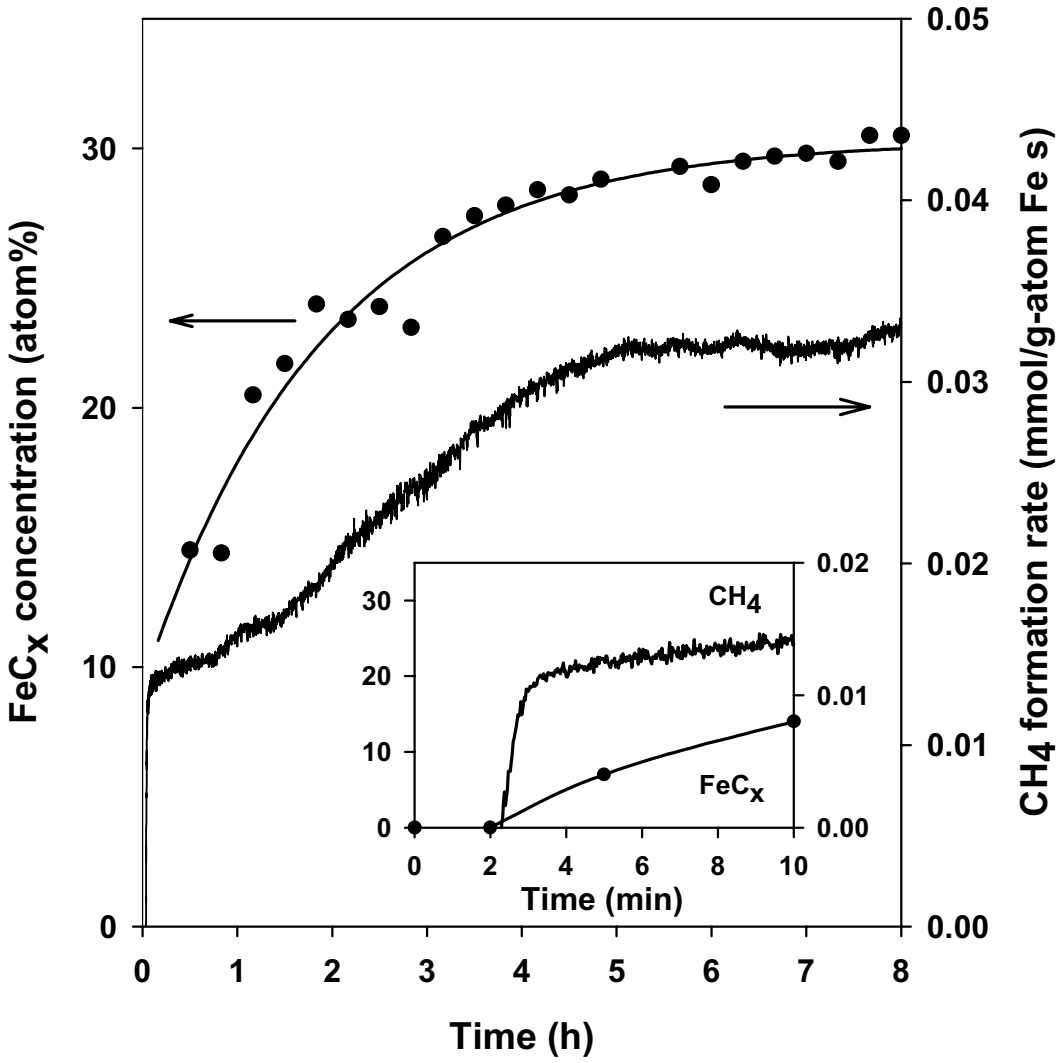

References

1. Storch, H. H.; Golumbic, N.; Anderson, R. B. *The Fischer-Tropsch and Related Synthesis*; John Wiley & Sons: New York, 1951.
2. Dry, M. E. In *Catalysis: Science and Technology*; Anderson, J. R., Boudart, M., Ed.; Springer Verlag: New York, 1981; Vol. 1, Chapter 4.
3. Iglesia, E.; Reyes, S. C.; Madon, R. J.; Soled, S. L. *Advances in Catalysis*; Academic: 1993; Vol. 39.
4. Iglesia, E. *Appl. Catal. A: General* **1997**, *161*, 59.
5. Dwyer, D. J.; Somorjai, G. A. *J. Catal.* **1978**, *52***,** 291.
6. Reymond, J. P.; Meriaudeau, P.; Teichner, S. J. *J. Catal.* **1982**, *75*, 39.
7. Kuivila, C. S.; Stair, P. C.; Butt, J. B. *J. Catal.* **1989**, *118*, 299.
8. Shultz, J. F.; Hall, W. K.; Dubs, T. A.; Anderson, R. B. *J. Am. Chem. Soc.* **1956**, *28*, 282.
9. Dictor R.; Bell, A. T. *J. Catal.* **1986**, *97*, 121.
10. Rao, K. R. P. M.; Huggins, F. E.; Mahajan, V.; Huffman, G. P.; Rao, V. U. S.; Bhatt, B. L.; Bukur, D. B.; Davis, B. H.; O'Brien, R. J. *Topics in Catal*. **1995**, *2*, 71.
11. Mansker, L. D.; Jin, Y.; Burker, D. B.; Datye, A. K. *Appl. Catal. A: General* **1999**, *186*, 277.
12. Amelse, J. A.; Butt, J. B.; Schwartz, L. H. *J. Phys. Chem. B* **1978**, *82*, 558.
13. Lindner, U.; Papp, H. *App. Surf. Sci.* **1988**, *31*, 75.
14. Shroff M. D.; Kalakkad, D. S.; Coulter, K. E.; Kohler, S. D.; Harrington, M. S.; Jackson, N. B.; Sault, A. G.; Datye, A. K. *J. Catal.* **1995**, *156*, 185.
15. Sayers, D. E.; Bunker, B. A. In *X-Ray Absorption: Principles, Applications, Techniques of EXAFS, SEXAFS and XANES*; Koningsberger, D. C., Prins, R., Ed.; John Wiley and Sons: New York, 1988.
16. Malinowski, E. R.; Howery, D. G. In *Factor Analysis in Chemistry;* John Wiley & Sons: New York, 1981.
17. Meitzner, G. D.; Huang, E. S. *Fresenius J. Anal. Chem.* **1992**, *342*, 61.
18. Ernst, B.; Bensaddik, A.; Hilaire, L.; Chaumette, P.; Kiennemann, A. *Catal. Today* **1998**, *39*, 329.
19. Clausen B. S. *Catal. Today* **1998**, *39*, 293.
20. Anderson, R. B.; Hofer, L. J. E.; Cohn, E. M.; Steiner, H.; Greyson, M.; Weller, S. W.; In *Catalysis*; Emmett, P. H., Ed.; Reinhold: New York, 1956; Vol. 4.
21. Li, S.; Li, A.; Iglesia, E.; to be submitted to *J. Catal.*
22. Barton, D. G.; Ph. D dissertation, University of California, Berkeley, 1998.
23. Bearden A.; Burr, A. F.; *Rev. Mod. Phys.* **1967**, *39*, 125.
24. WinXAS97 is an XAS data analysis program for PCs running MS-Windows by Thorsten Ressler (http://ourworld.compuserve.com/homepages/t_ressler).
25. Li, S.; Meitzner, G. D; Iglesia, E; to be submitted to *J. Catal.*
26. Köbel, H.; Ralek, M. *Catal. Rev. Sci. Eng.* **1980**, *21*, 225.
27. Oyama, S. T.; Schlatter, J. C.; Metcalfe, J. E. III; Lambert, J. M. Jr.; *Ind. Eng. Chem. Res.* **1988**, *27*, 1639.
28. Kapoor, R; Oyama, S. T. *J. Mater. Res.*, **1997**, *12*, 471.
29. Lide, D. R.; Frederikse, H. P. R., Ed.; *Handbook of Chemistry and Physics*, 75th Ed.; The Chemical Rubber Company press: Boca Raton, 1994.
30. Kung, H. H. *Transition Metal Oxides: Surface Chemistry and Catalysis*; In *Studies in Surface Science and Catalysis*; Kung, H. H. Ed.; Elsevier: New York, 1989; Vol. 45.

4.3. Structural Analysis of Unpromoted Fe-Based Fischer-Tropsch Catalysts Using X-Ray Absorption Spectroscopy

Abstract

The structure of unpromoted precipitated Fe catalysts was determined by Mössbauer emission and X-ray absorption spectroscopies after use in the Fischer-Tropsch synthesis (FTS) reaction for various periods of time in well-mixed autoclave reactors. X-ray absorption near-edge spectroscopy (XANES), extended X-ray absorption fine structure (EXAFS) analysis, and Mössbauer spectroscopy showed consistent trends in the structural evolution of these catalysts during reaction. The nearly complete formation of Fe carbides during initial activation in CO was followed by gradual re-oxidation to form Fe_3O_4 with increasing time on stream. Fe_3O_4 became the only detectable Fe compound after 450 h. The observed correlation between FTS rates and Fe carbide concentration, and the unexpected re-oxidation of the catalysts as CO conversion decreased, suggest that the deactivation of Fe catalysts in FTS reactions parallels the conversion of Fe carbides to Fe_3O_4. It appears that the CO activation steps responsible for replenishing carbidic surface species and for removing chemisorbed oxygen are selectively inhibited by deactivation of surface sites, leading to the oxidation of Fe carbide even in the presence of a reducing reactant mixture.

1. Introduction

Iron oxide precursors activated to form complex mixtures of carbides and oxides have been widely used as Fischer-Tropsch synthesis (FTS) catalysts since their initial commercial use [1]. Currently, they are used in industrial practice by Sasol (~ 110,000 bbl/day) and Mossgas (~ 30,000 bbl/day) [2,3]. These Fe catalysts are treated in H_2, CO, or H_2/CO in order to convert the starting Fe oxide precursors into active FTS catalysts. These Fe oxide precursors can be partly [4] or completely [5] reduced to Fe metal by treatment in H_2 using various protocols [5,6]. The sample may also be reduced and converted to iron carbides using CO as the reducing and carburizing agent [7,8]. Synthesis gas can also be used as the activating reagent. Activation in synthesis gas is usually started at temperatures well below typical FTS reaction temperatures, and then the temperature is gradually increased to typical FTS reaction temperatures [9-19].

The activation of Fe-based precursors in synthesis gas is a complex process that is difficult to follow as it occurs. The effects of the structural changes that occur during activation on the catalytic behavior of these materials remain unclear. For example, as the partial pressure of hydrogen increases relative to that of CO during activation, at otherwise similar conditions, the ultimate steady-state FTS rates decrease [20]. Promoters, such as Cu and K, shorten the time required for the conversion of Fe oxide precursors into active catalysts. After the initial activation, the structure of Fe-based FTS catalysts continues to evolve with increasing time on stream [21].

X-Ray absorption near-edge spectroscopy (XANES) and extended X-ray absorption fine structure (EXAFS) methods provide unique information about the oxidation state and local environment of each absorber element in complex multi-component materials. In this study, these techniques were used in order to determine the structure of Fe catalysts after they catalyze FTS reactions for various periods of time. In the initial studies reported here, an unpromoted precipitated iron catalyst was used in order to avoid the complexity introduced by chemical and structural promoters. The X-ray absorption results were compared with previous Mössbauer spectroscopy data [13,21] on similar Fe catalysts and the results of these two structural characterization techniques are taken together with their catalytic properties at a given time on stream in order to infer the nature of the active species and the chemical and structural changes that accompany deactivation during FTS reactions.

2. Experimental

2.1. Catalyst preparation procedures

One sample of the unpromoted Fe oxide precursor (Sample 0) and samples of this precursor after activation (Sample 1) and after use for various lengths of time (Samples 3, 5, 7, 10, 13, 19, 20) were examined. The Fe oxide precursor was prepared by precipitation from an aqueous solution of $Fe(NO_3)_3 \cdot 9H_2O$ (Johnson Matthey Co., 98+% metals basis, 1 M; 157 cm^3/min) using concentrated NH_4OH (VWR, reagent grade, 28-30 wt.%; 71 cm^3/min). The pH of the slurry was kept constant at 9.3 and the residence time in the reactor was 300 s. This resulted in a total slurry volume of 34.4 liters. After initial filtration, the precipitates were washed by re-slurring twice with 34.4 liters of deionized water with intervening filtration using rotary drum filters.

The washed precipitates were dried in air at 373 K overnight. The dried materials were ground using a mortar and pestle in order to obtain particles with ~0.15 mm diameter and then treated in stagnant dry air at 623 K for 4 h.

2.2. Activation and FTS reactions

All FTS experiments were carried out in a 1-liter continuous stirred tank reactor (CSTR). The catalyst precursor (64.44 g) was suspended in C-30 oil (Ethylflow, decene trimers; Ethyl Corp., 290 g) and pretreated with CO at 543 K and 1.22 MPa for 24 h. The CO flow (58.7 sl/h g-Fe) was started at ambient conditions (298 K and 0.1 MPa), the pressure was raised to 1.22 MPa, and the temperature of the reactor was then increased to 543 K at 2 K/min and maintained at this temperature for 24 h. Following this activation treatment, the reactor was brought to reaction conditions (543 K, 1.22 MPa, $H_2/CO = 0.68$, 3.1 sl $(CO+H_2)$/h g-Fe) by introducing H_2 into the CO stream over a period of ~3 h.

Reaction products were analyzed using gas chromatography. Gas products were analyzed using a Hewlett-Packard Quad-Series Refinery Gas Analyzer (QRGA). The analysis of the aqueous phase collected after the reactor was carried out using a Hewlett-Packard 5790 gas chromatograph equipped with a thermal conductivity detector and a Porapak Q column. Oil and wax were combined and analyzed with a Hewlett-Packard 5890 gas chromatograph equipped with a flame ionization detector and a 60 m DB-5 column. The wax products were analyzed on a Hewlett-Packard 5890 high temperature gas chromatograph using flame ionization detection and a 30 m alumina clad HT-5 column.

Catalyst samples were extracted from the autoclave during reaction using a dip tube blanketed with an inert gas. All subsequent handling of the used catalysts was carried out under inert gas within a glove box. A total of 20 samples were withdrawn from the reactor during the 452 h experiment. The conversions have not been corrected for the decline in the amount of catalyst withdrawn from the reactor. Based upon the initial solid content of the slurry, the initial slurry volume, and the amount of sample removed from the reactor, catalyst removal would account less than a 15% decrease in CO conversion by the end of the experiment.

2.3. Mössbauer emission spectroscopy measurement

The Mössbauer experiments used a constant acceleration spectrometer. The radioactive source comprised of 50 mCi of ^{57}Co in a Rh matrix. Samples 1, 3, 10, and 20 in powdered form were loaded into Plexiglass compression holders presenting a thin sample to the beam. Spectra collected from Samples 1, 3 and 10 were analyzed by least squares fitting the data to a summation of five sextets, while the spectrum collected from Sample 20 was fitted to the sum of two sextets. Hyperfine parameters extracted from the fits were used to identify the composition of the samples. The two sextets having the highest hyperfine magnetic field were found to correspond to Fe at the tetrahedral and the octahedral sites of Fe_3O_4. The remaining three sextets were found to correspond to Fe centers located at the three crystallographic sites in the Hägg carbide (Fe_5C_2).

2.4. X-absorption sample preparation

Fe K-edge X-ray absorption spectra for standard Fe compounds, for the fresh sample (Sample 0), and for four used Fe catalysts (Samples 5, 7, 13, 19) were measured. Fe_2O_3 (Alfa AESAR, 99.998%), Fe_3O_4 (Alfa AESAR, 99.998%) and FeO (Alfa AESAR, 99.5%) were used as standards for the fitting of the near-edge (XANES) spectra of catalyst samples. Fe carbides (FeC_x), which may form during FTS, were prepared by temperature-programmed reaction (0.167 K/s to 973 K) of precipitated Fe_2O_3 (0.2 g) in flowing CO (Matheson, 99.99%, 100 cm^3/min) [22]. The resulting FeC_x was passivated using 1% O_2 in He (Matheson, 99.999%, 20 cm^3/min) for 1 h before removing from the synthesis cell and measuring its spectrum. All samples, including standard compounds and catalyst samples, were mixed and finely ground with graphite powder (Alfa AESAR, 99.9995%), affixed onto a plate window, and sealed with Kapton films before XAS measurements. The Fe content in samples was kept at ~10 wt.% Fe in order to minimize the attenuation of the incident beam and to avoid distortion of the spectra.

2.5. X-ray absorption spectroscopy (XAS) measurements

X-ray absorption spectra were measured at the Stanford Synchrotron Radiation Laboratory (SSRL). Fe K-edge absorption data were acquired on a wriggler side-station (beamline 4-3) with the storage ring operated at 30-100 mA and 3.0 GeV. The beam resolution was better than 2.0 eV at the Fe K-edge (7.112 keV) [23]. Two Si(111) single crystals were used in the monochromator, which was detuned by 20% in order to eliminate higher order harmonics from the beam. A 1.25×15 mm beam was allowed to pass through the samples, which were held in a plate window by a Kapton film. N_2-filled ion chamber detectors were used to measure the intensities of the X-ray beam entering the sample (I_o), after the sample (I_1), and after a 5 μm Fe calibration foil (I_2). The sample spectrum (I_1/I_2) and the reference spectrum (I_1/I_2) were obtained simultaneously in transmission mode.

2.6. X-Ray absorption data analysis procedures

X-ray absorption spectra were analyzed using WinXAS (version 1.2) [24]. Raw spectra were shifted in order to align the first inflection point in the Fe foil reference spectrum with the known absorption energy of Fe metal (7.112 keV) [23]. Linear fits to the pre-edge region (6.900-7.100 keV) were subtracted from the spectra and the post-edge background was normalized using a six-order polynomial (7.240-8.112 keV). Principal component analysis [25] and linear combination methods [26] were used in order to obtain the phase composition of materials using the near-edge region (7.090-7.240 keV). The EXAFS data were analyzed after background subtraction using Fourier transforms in the range from 2.5 to 16 $Å^{-1}$.

3. Results

3.1. Mössbauer structural analysis

Table 1 shows the catalyst composition and the relative areal fraction of their sextets obtained from the Mössbauer spectra as a function of time on stream. It is worth noting here that these areal fractions measured at room temperature were not corrected by using the recoil-free fraction ratio of the different Fe sites. Therefore, the fractional composition of the samples might be slightly different from the areal fractions. The Fe_5C_2 phase was established from the measured

hyperfine parameters, although the measured fraction ratio (Fe_I:Fe_{II}:Fe_{III}) did not conform to the expected ratio of (2:2:1). In large-crystal Fe carbide samples, the ratio frequently differs from (2:2:1) because of the variable concentration of carbidic carbon. Here, however, the deviation is stronger and indicates that crystallization is incomplete. In spite of this, Fe_5C_2 is the only iron carbide that can be discerned from the Mössbauer measurements. The Mössbauer data (Table 1) show that the extent of carburization was nearly complete after the 24 h activation period in contact with flowing CO, and then decreased with time on stream. After 452 h, only Fe_3O_4 was detected.

3.2. Fe K-edge XANES

Figure 1 shows X-ray absorption near-edge spectra (XANES) for Samples 0, 5, 7, 13, and 19. All spectra show weak pre-edge peaks, indicating the presence of some residual Fe oxides. The absorption edge energy, defined at the first inflection point in the absorption edge, shifts to lower energies for Samples 5 and 7, suggesting the formation of Fe species with lower oxidation states than in Fe_3O_4. The absorption energy shifts back to higher values for Samples 13 and 19. The higher absorption energies on the catalyst precursor (Sample 0) and in Samples 13 and 19 and the more intense pre-edge and absorption features in the near-edge region indicate the more prevalent presence of Fe oxides in these samples compared to the other used samples.

Principal component analysis (PCA) identified only Fe_3O_4 and FeC_x in Samples 5-19. The near-edge spectra for these samples can be described as a combination of the standard spectra for Fe_3O_4 and FeC_x; the relative amounts of these two phases can be obtained using least square error minimization techniques [26]. Fe_2O_3, FeO and Fe were excluded from the fittings because they were rejected by PCA and because their presence failed to improve the fit.

The XAS spectra of the catalyst precursor before activation cannot be fitted to combinations of Fe_2O_3 and Fe_3O_4 spectra. The EXAFS of this sample (Sample 0) suggests the presence of FeO(OH), apparently as a result of the incomplete crystallization of the oxides during calcination at relatively low temperatures. These temperatures (623 K) are generally sufficient to decompose FeO(OH), but the short treatment time and the stagnant nature of the ambient air within and above the sample bed appeared to inhibit water removal and dehydration, and led to amorphous Fe oxides. Therefore, Sample 0 contained hydrated Fe oxides, which did not crystallize fully during synthesis. X-ray diffraction (XRD) and Mössbauer analyses of other samples that received a similar activation are consistent with these conclusions.

Table 2 shows the relative abundances of standard compound structures corresponding to the best fits of the experimental spectra for each sample. Figure 2 presents a typical fit to the spectrum for Sample 5. All the fits were excellent. The results from linear combination fits show a monotonic decrease in the relative abundance of Fe carbides with increasing time on stream (Samples 5, 7 and 13). After FTS reactions for 432 h, the only detectable phase was Fe_3O_4 (Sample 19), as also found by Mössbauer emission spectroscopy.

3.3. Fe K-edge fine structure

Figure 3 shows the Fourier transforms of the Fe K-edge fine structure for each sample and for the standard Fe compounds. The radial structure function for the catalyst precursor (Sample 0) is poorly resolved, indicating a disordered or non-uniform geometry around Fe absorbers. The radial structure functions for Samples 5 and 7 appear to reflect the combined contributions of Fe_3O_4 and FeC_x. The relative contributions of these two structures suggest that Sample 5 has a higher Fe carbide fraction than Sample 7. After 264 h on stream, the catalyst (Sample 13) shows a fine structure similar to that of pure Fe_3O_4; after 432 h, the fine structure features in Sample 19 are identical to those in pure Fe_3O_4. The evolution of the radial structure function with increasing time on stream is consistent with the changes in structure detected from the linear combination analysis of the near-edge spectra.

3.4. Comparison of the results from Mössbauer emission and X-ray absorption spectroscopy

The quantitative phase compositions obtained from Mössbauer emission and X-ray absorption spectroscopies differ (Figure 4); the compositional trends obtained by the two techniques, however, are very similar. Both techniques show that the carbide phase is more prevalent in the earlier stages of contact with synthesis gas and that the Fe carbide content decreases with increasing reaction time; after about 400 h, the only detectable phase is Fe_3O_4. Both techniques indicate that the decrease in the amount of Fe carbide parallels the observed decrease in catalytic activity (Figure 4). Two possible explanations can be proposed for the quantitative differences in the carbide fractions obtained from the two spectroscopic techniques. The first is that the samples used for X-ray absorption spectroscopic measurements were stored for ~ 2 years. The samples were stored in the wax FTS product and under an inert gas blanket, but it is possible that some of the carbides were oxidized during storage, leading to the lower carbide fraction detected by XAS. Another possibility is that the Mössbauer technique overestimated the amount of the carbide phase present in the samples. The measured fractions of the oxide and the carbide were calculated from the areas of their sub-spectra divided by the area of the main spectrum, which included all sub-spectra. Corrections were not made for the fraction of the solid sampled by the Mössbauer technique, because such corrections require literature data for the recoil-free fraction of the oxide and carbide phases. Literature values are available for large crystals of these phases, but the small crystals present in FTS catalyst samples make such corrections non-rigorous.

4. Discussion

Integral Fischer-Tropsch synthesis rates decreased by almost a factor of ten, leading to a decrease in CO conversion from 86% to 12% after 452 h on stream (Figure 4). Clearly, the high conversions in the early stages of the reaction lead to much higher H_2O/H_2 and CO_2/CO ratios than those present at the low conversions prevalent at later reaction times. Thus, the oxidizing potentials of the reactant-product mixtures in the gas phase and in the liquid phases in equilibrium with this gas phase are significantly higher during the early stages of the experiment. Yet Fe carbides were the predominant Fe species at these conditions, although they decreased in relative abundance as the reaction proceeded for longer periods of time. In spite of the fact that CO_2 can lead to the oxidation of Fe carbides, the presence of added CO_2 ($CO_2/CO = 0.3$) in the feed gas did not influence CO conversion rates or apparently altered the structure of the catalytic phases. Thus, CO_2 was essentially inert at our reaction conditions. The addition of water at H_2O/CO ratios up to 0.3 also did not influence the rate of hydrocarbon formation, but it increased

the rate of water gas shift [27]. However, the lack of impact of added CO_2 and H_2O was studied only for an iron catalyst containing silica (4.4 atomic Si to 100 Fe) and potassium (1.0 atomic K to 100Fe). Thus, the extrapolation of these results to the unpromoted catalyst used in this study may not be appropriate.

It appears that individual iron particles undergo re-oxidation rather uniformly. If only the surfaces of each catalyst particle were rapidly oxidized during deactivation, and this initial process were followed by the slower oxidation of the bulk carbide phase, the CO conversion would decline much more rapidly than the concentration of the active Fe carbide phase. The experimental evidence indicates that both decline to a similar extent as deactivation occurs. Thus, it appears that catalyst particles start to re-oxidize via the nucleation of an oxide phase either at the surface or within their core, and ultimately re-oxidize completely, while other particles remain essentially as iron carbide. One possible explanation for this unusual behavior would be a distribution of carbide crystallites and a size-dependent thermodynamic propensity to re-oxidize, but data supporting such effects are not available and such particle size dependence would be unexpected for the large crystallites of Fe phases detected by X-ray diffraction. In any event, the bulk phase composition and specifically the relative abundance of Fe carbides in the unpromoted iron catalyst directly influence CO conversion rates (Figure 4). This is most readily explained if the catalyst system is composed of a mixture of catalyst particles whose surface resembles either iron oxide or iron carbide phases, and whose distribution favors less active Fe oxides over more active Fe carbides as the catalyst deactivates.

A tenuous balance among several concurrent processes determines the surface and bulk composition of a catalyst during steady-state Fischer-Tropsch synthesis. First, there must be a balance between the amount of CO that is converted to products in the Fischer-Tropsch and the water-gas shift reactions, and the amount of CO that is dissociated on the catalyst surface in a form that maintains the carbide phase. Any imbalance between these rates would lead to the net introduction or removal of carbon or oxygen atoms into the inorganic structure, and to the interconversion of Fe oxides and Fe carbides. If the removal of the carbon and oxygen atoms using hydrogen or CO becomes imbalanced, the surface chemical potential of either carbon or oxygen can become higher than in the contacting gas phase. This can lead to the formation of bulk structures in thermodynamic equilibrium with the steady-state surface chemical potential. On unpromoted iron catalysts, it appears that deactivation leads to the preferential inhibition of oxygen removal pathways over those leading to the removal of carbon to form CH_x species and ultimately hydrocarbons. The concomitant depletion of the surface carbon pool leads to the nucleation of Fe_3O_4 patches, which dissociate CO and catalyze FTS with very low reaction rates. If only the surface were oxidized, however, to resemble Fe_3O_4, the catalytic activity would change much more rapidly than the Fe oxide content in the catalysts and the catalyst would recarburize in the presence of the carburizing synthesis gas mixture present at low conversions. The catalytic activity declines at about the same rate as the bulk carbide phase. This eliminates the possibility of just surface oxidation causing the compositional changes defined by the Mössbauer and the X-ray absorption spectroscopy measurements and influencing FTS reaction rates.

In the case of the unpromoted Fe catalysts of this study, the re-oxidation may be caused, or at least initiated, by changes in the relative rates of oxygen formation in CO activation steps and of

oxygen removal by reaction with hydrogen or CO to form water and CO_2, respectively. Such changes occur concurrently with the observed decrease in the rate of the reaction, apparently because of the common need for H_2 activation steps for both monomer formation and for oxygen removal in FTS reaction catalyzed by Fe carbide particles. Thus, re-oxidation would reflects changes in the surface chemical potential of C*, O*, and H* adsorbed species, instead of corresponding changes in chemical potential within the contacting gas phase. In turn, this suggests that the removal of oxidizing species, such as adsorbed H_2O*, OH*, or O*, occurs via steps that are not quasi-equilibrated during FT synthesis, and that their surface concentrations can significantly exceed those that would be in equilibrium with the contacting gas phase. The non-equilibrated nature of water desorption steps has been recently demonstrated during FTS reactions on Co catalysts by the very low HD and D_2 concentrations among hydrogen molecules and by the low D-content in the hydrocarbon formed from $CO/H_2/D_2O$ reactant mixtures [28]

The data in Figure 4 suggest a direct relationship between the FTS rates and the concentration of Fe carbides during reaction. It appears that catalytically active species reside on carbided surfaces. Our recent studies have shown that Fe_3O_4 crystallites become almost immediately active in FTS reactions after exposure to synthesis gas and that only the incipient conversion of near surface oxide layers to Fe carbides is required for steady-state FTS rates [29]. Thus, the observed deactivation with time on stream is unlikely to reflect merely the bulk re-oxidation of a particle core to Fe_3O_4, because such particles would immediately re-activate to give high FTS reaction rates, as they initially do when Fe oxides precursors are activated in synthesis gas. Instead, it appears that the observed oxidation and deactivation of Fe carbides are concurrent processes caused by changes in the carbide surface, which render the oxidation potential of adsorbed species high enough to form Fe_3O_4 surfaces. These surfaces exhibit a structure or composition that prevents their re-carburization at FTS reaction conditions, even at the low conversion levels and reducing conditions prevalent as conversion decreases during catalyst deactivation.

5. Conclusions

Mössbauer and XAS measurements of the phase composition of unpromoted Fe catalysts sampled at various periods of FTS reactions showed a consistent decrease in the Fe carbide concentration with time on stream. The CO conversion decreased by a factor of 10 during the structural evolution of the catalysts from initial nearly pure Fe carbides after activation in CO, to their gradual oxidation with increasing reaction time, and their ultimate transformation to pure Fe_3O_4 after 450 h on stream. It appears that the observed oxidation and deactivation of Fe carbides are concurrent processes caused by changes of chemical potential of absorbed species at the carbide surface, which render higher concentrations of oxidizing species on the surface than in the contacting gas phase. These conditions, in turn, lead to the oxidation of Fe carbides even in the reducing environments prevalent as conversion decreases during catalyst deactivation.

Acknowledgments

This work was supported by the U.S. Department of Energy under Contract DE-FC26-98FT40308 and by the Commonwealth of Kentucky. X-Ray absorption data were collected at the

Stanford Synchrotron Radiation Laboratory (SSRL), which is operated by the U. S. Department of Energy, Office of Basic Energy Sciences, under Contract DE-ACO3-76SF00515.

Table 1. Mössbauer structural analysis results.

Sample	1	3	10	20
FTS reaction time (h)	0	23	168	452
Fe_5C_2 (atom %)	94	83	42	0
Fe_3O_4 (atom %)	6	17	58	100

Table 2. Linear combination of standard spectra fits to the sample XANES.

Sample	0	5	7	13	19
FTS reaction time (h)	-	71	121	264	432
FeC_x (atom %)	0	52	35	2	0
Fe_3O_4 (atom %)	-	48	65	98	100

Figure 1. Normalized Fe K-edge XANES for (A) Sample 0, (B) Sample 5, (C) Sample 7, (D) Sample 13, (E) Sample 19.

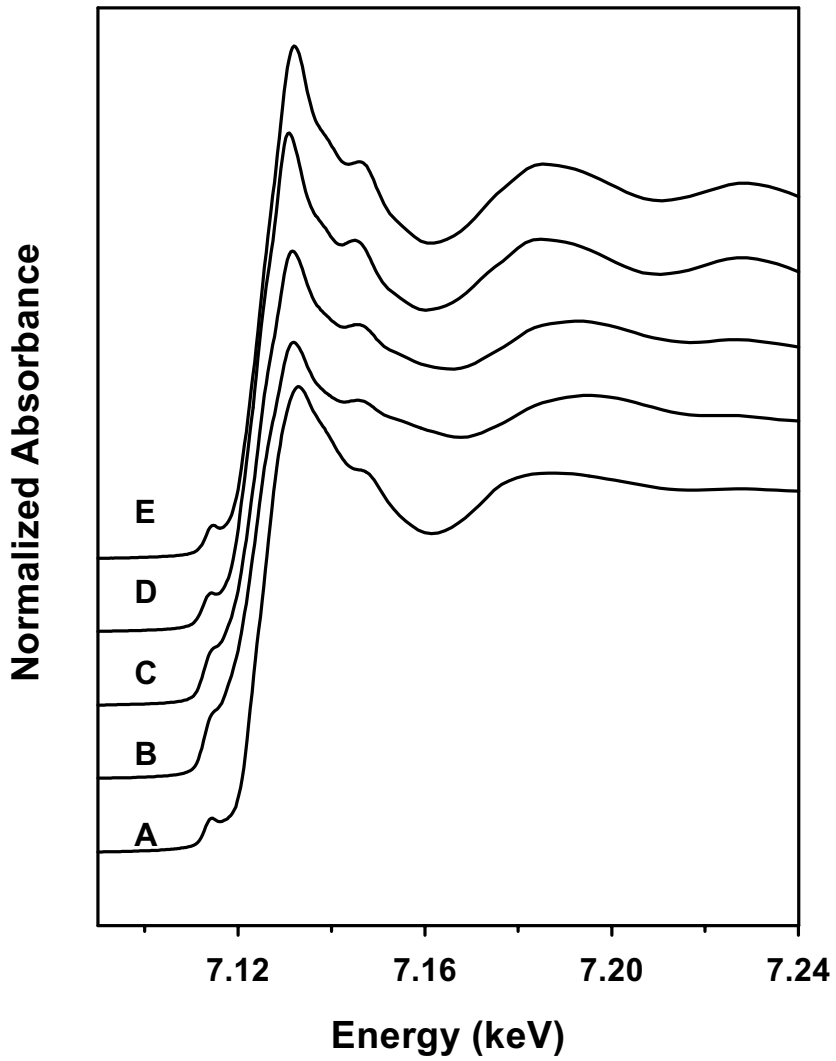

Figure 2. Experimental and the linear combination XANES fit for Sample 5.

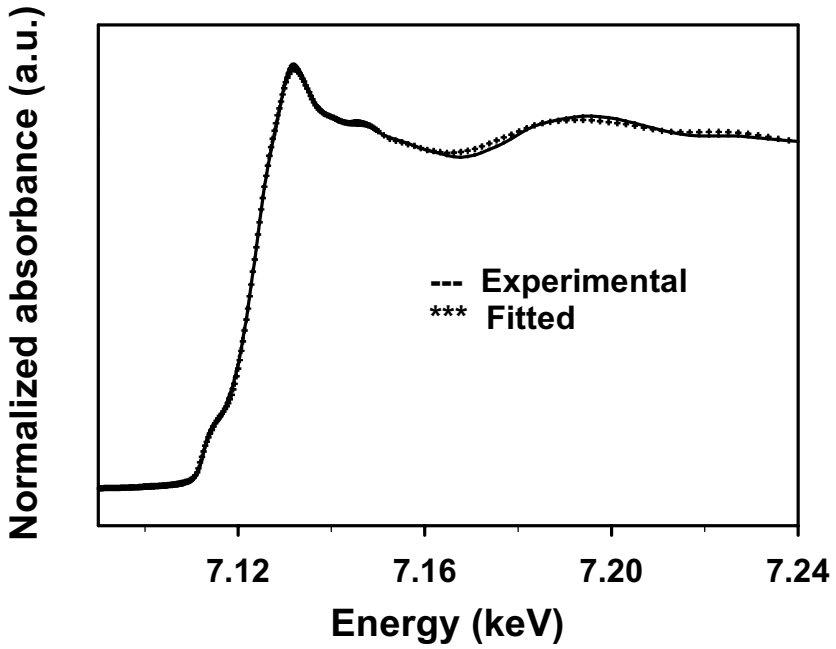

Figure 3. Fe K-edge EXAFS for (A) Sample 0, (B) Sample 5, (C) Sample 7, (D) Sample 13, (E) Sample 19, and standard compounds: Fe_2O_3 (triangle), Fe_3O_4 (cross), FeC_x (dot).

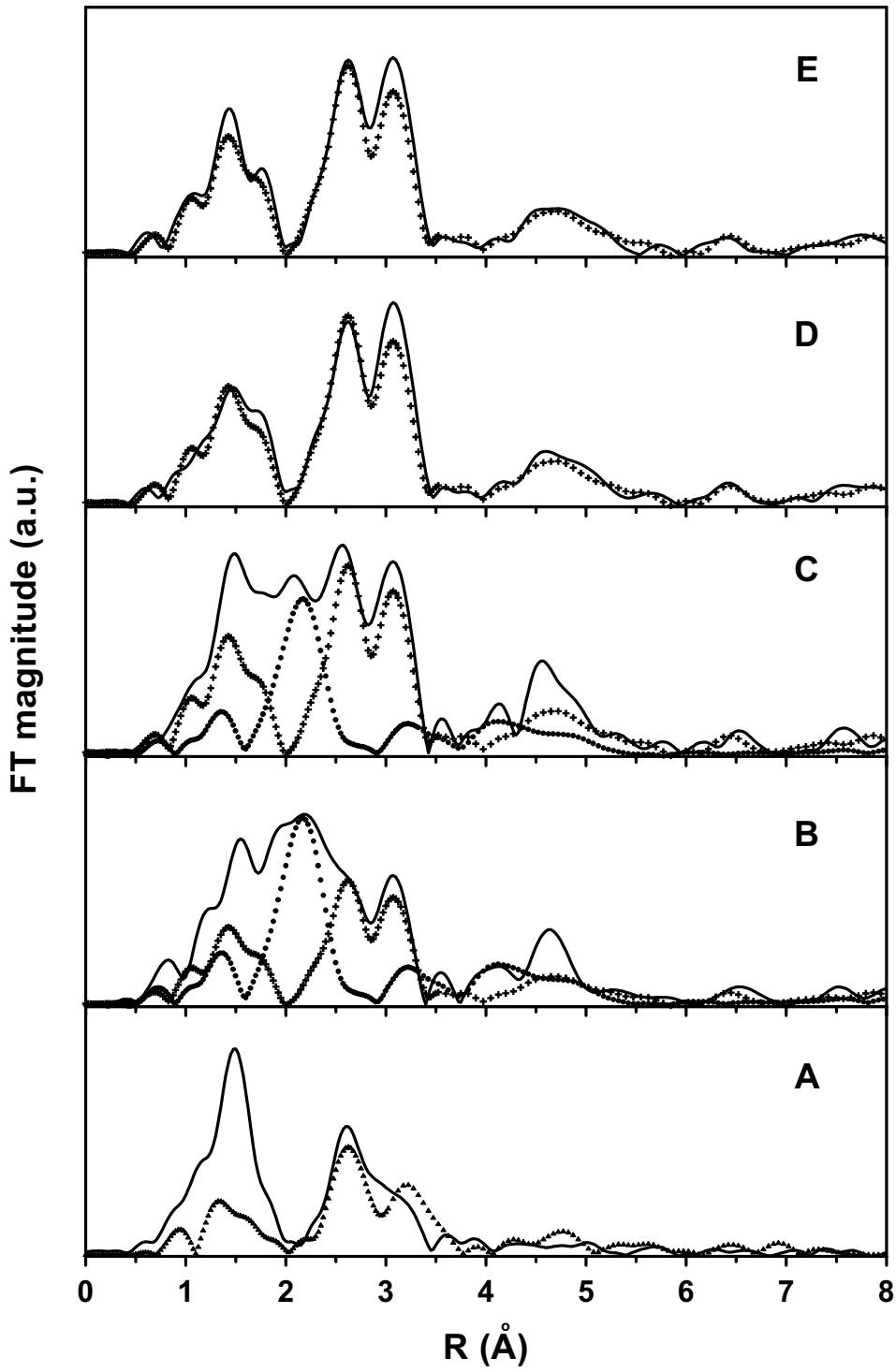

Figure 4. FTS rates measured from the CSTR (543 K, 1.22 MPa, $H_2/CO=0.68$, 3.1 sl$(CO+H_2)$/h g-Fe), and the Fe carbide concentrations obtained from the Mössbauer and the XAS measurements as a function of reaction time.

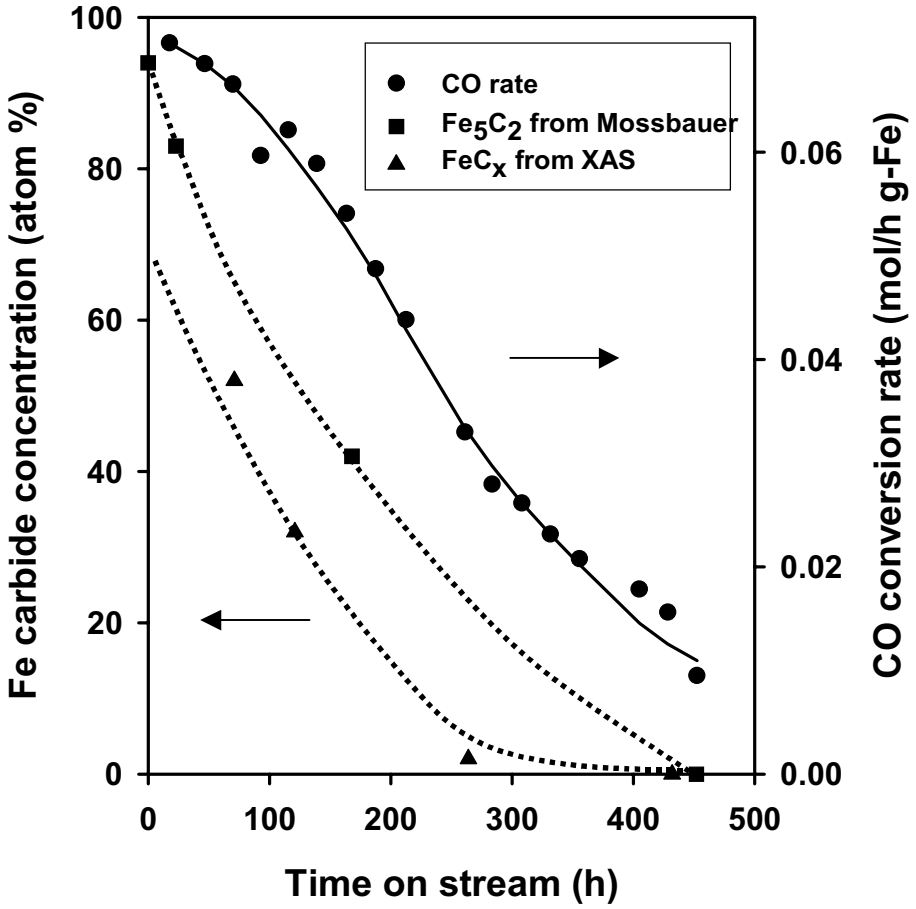

5. FISCHER-TROPSCH SYNTHESIS ON FE-BASED CATALYSTS

5.1 Effect of calcination temperature on the performance of Fe-Zn-Ru-K for FTS

During the current reporting period, FTS reactions were carried out on a Fe-Zn-Ru-K sample calcined at 673 K. We had previously reported the results of experiments conducted at deducing a comparison between Ru-promoted and Cu-promoted Fe-Zn samples [23]. However while the Cu-promoted samples were calcined at 673 K, the Ru-based samples had been subjected to pretreatment at 623 K. Our earlier studies with Fe-Zn-Cu-K samples had shown that samples calcined at lower temperatures had higher surface areas and higher FT rates [24]. The higher FT rates are likely to be due to the exposure of a larger number of Fe_xC crystallites at the catalyst surface. To check if a similar effect occurred in the case of the Ru-based samples when the pretreatment temperature is changed, a fresh batch of Fe-Zn-Ru-K (Zn/Fe=0.1, Ru/M=0.01, K/M=0.02, M=Zn+Fe) was prepared using a calcination temperature of 673 K.

A comparison of the data obtained on the Ru-promoted samples (623 K and 673 K) with the Cu-based sample (673 K) at 493 K and 31.6 bar, is shown in the following section. The CO conversion on these catalysts is shown as a function of reciprocal space velocity in Figure 5.1. The Ru-based samples have a higher activity than the Cu-promoted sample. A change in calcination temperature from 623 K to 673 K on Fe-Zn-Ru-K results in almost unchanged CO conversions.

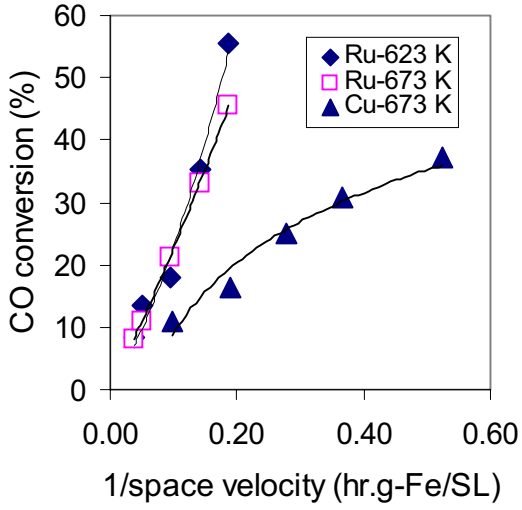

Figure 5.1 CO conversion as a function of reciprocal space velocity on Fe-Zn-Ru-K (Zn/Fe=0.1, Ru/M=0.01, K/M=0.02, M=Zn+Fe calcined at 623 K and 673 K), and Fe-Zn-Cu-K (Zn/Fe=0.1, Cu/M=0.01, K/M=0.02, M=Zn+Fe, calcined at 673 K); 493 K, 31.6 bar, $H_2/CO=2$.

The surface areas of the fresh Ru-K samples were 87 m^2/g and 71 m^2/g for calcination temperatures of 623 K and 673 K, respectively. However, it is conceivable that the differences in these surface areas could have been considerably reduced after the samples were subjected to carburization under FTS conditions. It has been previously shown that a promotion in the catalyst activity due to the presence of Ru is not the result of an additive effect caused by the

FTS rates on the Ru component. TPSR studies on Fe-Zn-Ru-K and Fe-Zn-Cu-K also showed that the presence of Ru on Fe-Zn promotes the reduction and carburization of Fe oxides more effectively than Cu, possibly as a result of the higher dispersion of the Ru component. Hence, the higher activity of the Ru-promoted samples compared to the Cu-based samples could be attributed to the better dispersion of the Fe_xC crystallites formed as a result of faster carburization on the catalyst surface, in the presence of Ru.

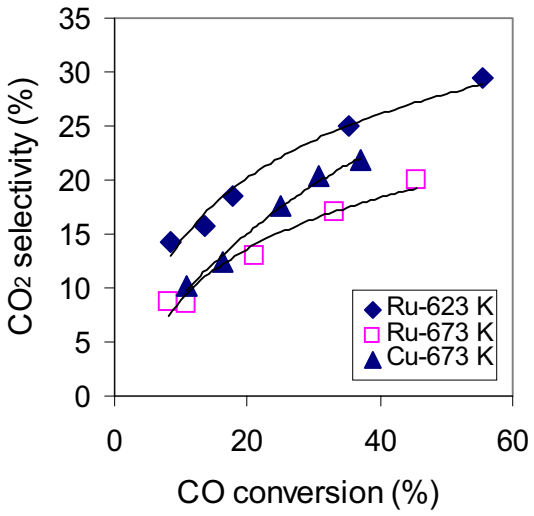

Figure 5.2 CO_2 selectivity as a function of CO conversion on Fe-Zn-Ru-K (Zn/Fe=0.1, Ru/M=0.01, K/M=0.02, M=Zn+Fe calcined at 623 K and 673 K), and Fe-Zn-Cu-K (Zn/Fe=0.1, Cu/M=0.01, K/M=0.02, M=Zn+Fe, calcined at 673 K); 493 K, 31.6 bar, $H_2/CO=2$.

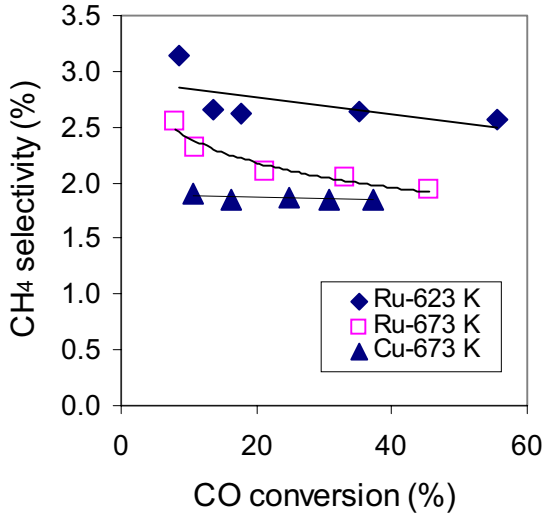

Figure 5.3 CH_4 selectivity as a function of CO conversion on Fe-Zn-Ru-K (Zn/Fe=0.1, Ru/M=0.01, K/M=0.02, M=Zn+Fe calcined at 623 K and 673 K), and Fe-Zn-Cu-K (Zn/Fe=0.1, Cu/M=0.01, K/M=0.02, M=Zn+Fe, calcined at 673 K); 493 K, 31.6 bar, $H_2/CO=2$.

The CO_2 and CH_4 selectivities for the Ru and Cu-promoted samples are shown as a function of CO conversion in Figures 5.2 and 5.3. The CO_2 and CH_4 selectivities appear to be slightly higher for the Fe-Zn-Ru-K sample calcined at 623 K than at 673 K. Since K has the ability to inhibit methane formation, the Cu-promoted sample has a lower methane content as it has a higher effective potassium-to-iron ratio than the Ru-promoted sample. The Ru-promoted samples calcined at 623 K and 673 K have BET surface areas of 87 and 71 m^2/g respectively. There exists the possibility that some hydrogenation sites may be present at the surface under reaction conditions on the higher surface area sample and these could lead to a small increase in the CH_4 selectivity. Differences in the CO_2 selectivities between the Ru and Cu samples are observed both in the primary (removal of CO as CO_2) and the secondary WGS reaction as indicated by the different slope and intercepts of all the curves in Figure 2. These are determined by the local concentrations of the individual species, i.e., C*, O*, H* and OH* on the catalyst surface.

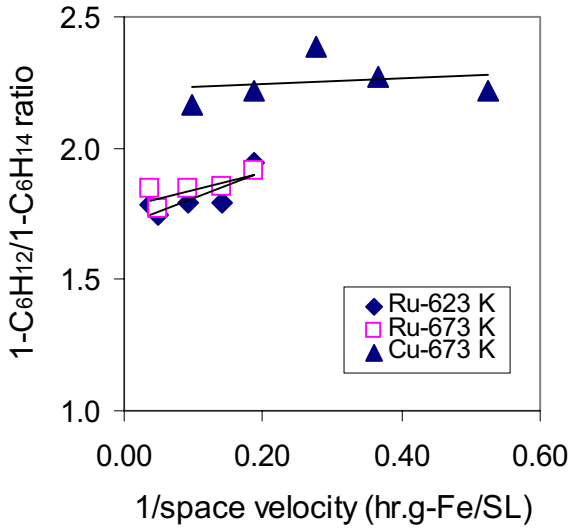

Figure 5.4. $1\text{-}C_6H_{12}/1\text{-}C_6H_{14}$ ratio as a function of reciprocal space velocity on Fe-Zn-Ru-K (Zn/Fe=0.1, Ru/M=0.01, K/M=0.02, M=Zn+Fe calcined at 623 K and 673 K), and Fe-Zn-Cu-K (Zn/Fe=0.1, Cu/M=0.01, K/M=0.02, M=Zn+Fe, calcined at 673 K); 493 K, 31.6 bar, $H_2/CO=2$.

1-hexene/*1*-hexane ratio for the different catalysts is shown as a function of space time in Figure 5.4. The Fe-Zn-Ru-K samples exhibit a higher olefin content than Fe-Zn-Cu-K. Since the Ru-based samples are likely to have a larger number of Fe_xC active sites, the ratio of K to Fe is lower for the Ru sample than the Cu sample and hence the olefin content is higher on the Cu-promoted sample rather than the Ru-promoted sample. A difference in calcination temperature does not show any noticeable change in the olefin content in the case of the Ru samples.

5.2 $^{13}CO_2$ addition studies on Fe-Zn-Cu-K

Experiments conducted with the addition of $^{13}CO_2$ to syngas on Fe-Zn-Cu-K, aimed at understanding the mechanism of CO_2 formation and the effect of CO_2 on FT rate and product selectivity, were delayed by difficulties associated with the GC-MS. The diffusion pump thermal switch in the MS had to be replaced. Currently tests are underway to check the use of a high molecular weight hydrocarbon solvent such as 1-hexadecane to dissolve the products on the low-pressure side of the backpressure regulator and separate them from CO and N_2. This would serve to concentrate the products and increase the sensitivity of the GC-MS towards the analysis of isotopic fractions. The experiments will be conducted at 508 K and 10 bar and will be completed within the next reporting period.

II. FISCHER-TROPSCH SYNTHESIS ON CO-BASED CATALYSTS

1. Preparation of a new batch of 21.9% Co/SiO_2 catalyst

In this reporting period a new batch of 21.9% Co/SiO_2 catalyst was prepared and tested.
even if the C_{5+} selectivity increases with increasing residence timeAbout 20 g were prepared by incipient wetness impregnation of SiO_2 (PQ Co. CS-2133) with Co nitrate (Aldrich 98%) solution. The samples were dried at 60°C for 48 h. Temperature-programmed reduction (TPR) was carried out in order to determine required pretreatment conditions for all catalyst precursors. In Figure 2.1 the results of the TPR are presented: Figure 2.1 – TPR of a 21.9% Co/SiO_2 catalyst

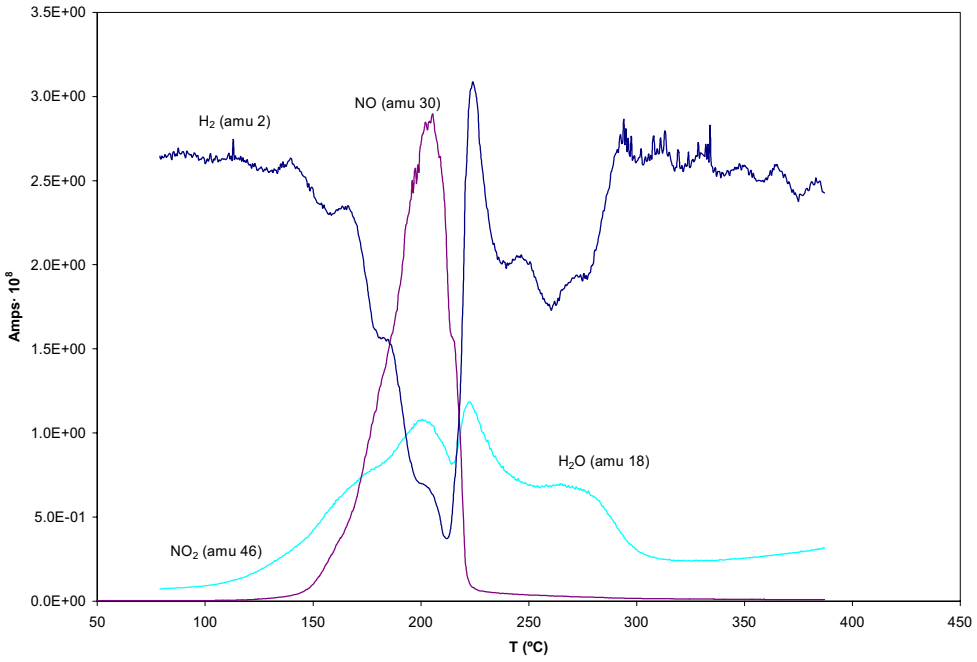

in particular it can be observed that the hydrogen consumption starts at about 160°C at which temperature some NO appears. This shows that the supported cobalt nitrate decomposes at that temperature.
The resulting cobalt oxide species reduce completely below 300°C. According to these data, the catalyst precursors were pretreated with the following procedure:

(1) reduced in flowing H_2 (20 ml min^{-1} g^{-1} cat) by increasing the temperature from 20°C to 150°C at 10°C min^{-1} and from 150°C to 350°C at 05°C/min (This low heating rate minimizes the deleterious effect of the water formed during the decomposition of Co nitrate and during the reduction of Co oxides, and it leads to higher Co dispersion)
(2) held at 350°C in flowing H_2 for 1 h, and cooled to 25°C
(3) passivated in a 1% O_2/He at 25°C before exposure to ambient air

The catalyst was tested by running experiments at various bed residence times. The results, in terms of CO conversion (x_{CO}) and selectivities are reported in Figure 2.2. The overall selectivity to olefins having from 2 to 12 carbon atoms (s_{Olef}) is also reported.

Activity and selectivities are similar to the ones measured on previous batches of catalyst.

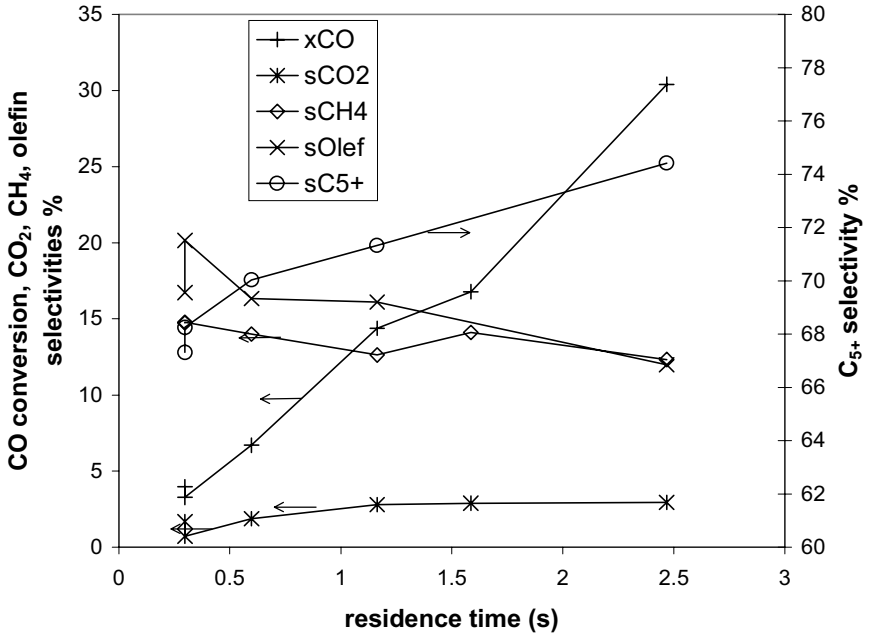

Figure 2.2 – Bed residence time run on a 21.9% Co/SiO_2 catalyst (T = 200°C; P = 20 bar; inlet $H_2/CO = 2$)

The selectivity to methane is actually slightly too high for the lowest residence times: this could be due to a change in the response factors of the columns of the GC. Also, even if the C_{5+} selectivity increases with increasing residence time, the selectivity to methane shows no significant decrease.

2. Transient experiments with Co/SiO_2 catalysts

During the current period, switching experiments were started in the Co-FTS unit after the required modifications were implemented. Switching from synthesis gas to hydrogen under reaction conditions, while measuring the CH_4 transient, will provide information about the number of active sites on the catalyst. Similar studies conducted in the presence of water will be used to discern whether the enhancing effect of water on FTS rates and C_{5+} selectivity is caused by the participation of water in rate-determining elementary steps, or by reactions of water with unselective and less reactive carbon pools on Co surfaces.
A mass spectrometer (Laybold Inficon, Transpector series) was hooked up to the reactor outlet before the hot trap in order to monitor the product transient. As a first step in this study, a blank run was conducted by switching between synthesis gas to hydrogen in an empty reactor. This test was conducted in order to determine if there was dispersion in the reactor even in the absence of a catalyst. The test was run at room temperature and 8.6 bar. The flow to the reactor of syngas before the switch, and of hydrogen afterwards, was maintained identical (about 100 cc/min), in order to avoid pressure losses after the switch. The switch was operated after the signal of mass

28 and mass 2 had reached a steady signal. The transient thus obtained is reported in Figure 2.3: it can be observed that this system is capable of measuring the details of the transient with excellent accuracy.
Yet there seems to exist some small diffusion problems of syngas which may be retained in some stagnant pockets in the lines before the reactor inlet. This can be suggested by the change in slope of the ascending H_2 signal and of the descending syngas signal, indicated in Figure 2.3. Some stagnant syngas in any dead volume before the entrance to the reactor can in fact diffuse in the hydrogen rich gas flowing after the switch, thus decreasing the velocity of the detected response.

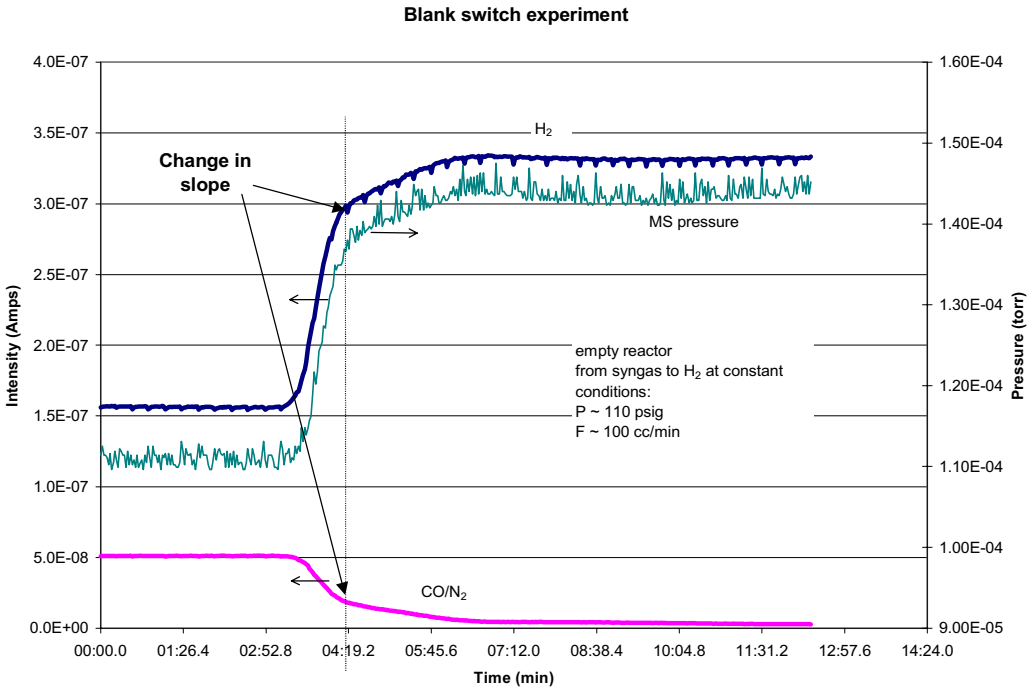

Figure 2.2 – Blank switch experiment: from syngas to hydrogen at room temperature and high pressure

In order to improve the hydrodynamics, the switching valve will be moved as close to the reactor as possible. Next, such studies will be conducted with a catalyst on-stream and the results will be presented in the upcoming period. These chemical transient studies will be followed by more challenging isotopic transient studies, in which switching between $H_2/^{12}CO$ and $H_2/^{13}CO$ will be used to count the number of active CO species during steady-state FTS reaction.

3. In situ FTIR Studies to Study the Water Effect

In situ FTIR spectra are being collected on a 21.9% Co/SiO_2 catalyst at FTS reaction conditions (i.e., 473 K and 5 atm). These studies will help probe the potential role of water in the FTS reaction, i.e., if water enhances reactivity by reacting with inactive or less reactive carbon pools on the Co/SiO_2 surface. This information will be gathered by the observation of the IR bands in

the 1900-2200 cm^{-1} region corresponding to the absorption of CO, both in the presence and absence of water. These experiments will be completed within the next quarter.

II. APPENDIX

1. References

1. M. E. Dry, The Fisher-Tropsch Synthesis, in *Catalysis-Science and Technology*, Vol. 1, p. 160, J. R. Anderson and M. Boudart eds., Springer Verlag, New York, 1981.
2. F. Fischer and H. Tropsch, *Brennstoff-Chem.* 7 (1926) 97.
3. R. B. Anderson, in *Catalysis* Vol. 4, p. 29, P. H. Emmett eds., Van Nostrand-Reinhold, New York, 1956.
4. H. H. Storch, N. Golumbic and R. B. Anderson, *The Fischer-Tropsch and Related Syntheses*, Wiley, New York, 1951; R. B. Anderson, *The Fischer-Tropsch Synthesis*, Wiley, New York, 1984.
5. H. Kolbel and M. Ralek, *Catal. Rev.-Sci. Eng.* 21 (1980) 225.
6. J. W. Niemantsverdriet and A. M. van der Kraan, *J. Catal.* 72 (1981) 385.
7. J. A. Amelse, J. B. Butt and L. J. Schwartz, *J. Phys. Chem.* 82 (1978) 558.
8. G. B. Raupp and W. N. Delgass, *J. Catal.* 58 (1979) 348.
9. R. Dictor and A. T. Bell, *J. Catal.* 97 (1986) 121.
10. J. P. Reymond, P. Meriaudeau and S. J. Teichner, *J. Catal.* 75 (1982) 39.
11. C. S. Kuivila, P. C. Stair and J. B. Butt, *J. Catal.* 118 (1989) 299.
12. C. S. Huang, L. Xu and B. H. Davis, *Fuel Sci. Tech. Int.* 11 (1993) 639.
13. S. Soled, E. Iglesia and R. A. Fiato, *Catal. Lett.* 7 (1990) 271.
14. S. Soled, E. Iglesia, S. Miseo, B. A. DeRites and R. A. Fiato, *Topics in Catal.* 2 (1995) 193.
15. E. Iglesia, A research proposal submitted to the Division of Fossil Energy.
16. R. J. O'Brien, L. Xu. R. L. Spicer and B. H. Davis, *Energy and Fuels*, 10 (1996) 921.
17. D. B. Bukur, D. Mukesh, and S. A. Patel, *Ind. Eng. Chem. Res*., 29, 194 (1990).
18. 1st Quarterly report, 1999. U.S. Department of Energy under contract # DE-FC26-98FT40308.
19. 2nd Quarterly report, 1999. U.S. Department of Energy under contract # DE-FC26-98FT40308.
20. 3rd Quarterly report, 1999. U.S. Department of Energy under contract # DE-FC26-98FT40308.
21. 4th Quarterly report, 1999. U.S. Department of Energy under contract # DE-FC26-98FT40308.
22. 1st Quarterly report, 2000. U.S. Department of Energy under contract # DE-FC26-98FT40308.
23. 2nd Quarterly report, 2000. U.S. Department of Energy under contract # DE-FC26-98FT40308.
24. 3rd Quarterly report, 2000. U.S. Department of Energy under contract # DE-FC26-98FT40308.
25. 4th Quarterly report, 2000. U.S. Department of Energy under contract # DE-FC26-98FT40308.

2. Abstract for the 17th North American Catalysis Society (NACS 2001) Meeting

Structural Evolution and Site Requirements for Fischer-Tropsch Synthesis Catalysts Based on Fe Oxide Precursors Promoted with Cu, Ru, or K

Senzi Li, Sundaram Krishnamoorthy, Anwu Li, and Enrique Iglesia
Department of Chemical Engineering, University of California,
Berkeley, CA 94720

The effects of different promoters (Ru, Cu, ZnO, and K_2CO_3) on the density and structure of active sites for the Fischer-Tropsch synthesis (FTS) was studied. The structure, reduction and carburization behavior, and catalytic properties of the catalysts were examined using a combination of isothermal kinetic transient and spectroscopic methods including on-line mass spectroscopy, *in situ* X-ray absorption spectroscopy, and steady-state FTS catalytic rate measurements. Isotopic jump and site titration methods were used to estimate the density of active sites, to establish the identity and reversibility of elementary steps, and to confirm the structure-function rules suggested by the kinetic and spectroscopic methods.

Fe-based catalysts were prepared by co-precipitation of Fe and Zn (Zn/Fe=0.1) nitrates with $(NH_4)_2CO_3$ to form porous mixed oxides, which were subsequently impregnated with Cu (Ru) nitrate or K carbonate solutions (M/Fe=0-0.04, M=Cu, K, or Ru), similar to the procedure used in another study [1]. Displacing intrapore water with alcohol before drying the precipitate and decreasing the treatment temperature from 673 K to 543 K increased the surface area of Fe-Zn-K-Cu oxides from 65 to 120 m^2/g. These procedures appear to prevent pore mouth pinching during by decreasing the surface tension of intrapore liquids.

The reduction of Fe_2O_3 to Fe_3O_4 in H_2 in Fe-Zn-K-Cu (Ru) precursors is faster than on Fe-Zn-K samples; Cu and Ru reduce at low temperatures and provide H_2 dissociation sites unavailable on Fe_2O_3. Oxygen removal and carbon introduction rates during exposure of Fe-Zn-K-Cu (Ru) oxides to CO showed that such processes occur sequentially via Fe_2O_3 reduction to Fe_3O_4, incipient removal of a minority of the O-atoms in Fe_3O_4, and rapid carburization of such oxygen-deficient species to form a χ-$Fe_{2.5}C$ and θ-Fe_3C mixture at 540 K or pure θ-Fe_3C at around 720 K. Cu and Ru increased the rate of oxygen removal from Fe_2O_3 and Fe_3O_4 and thus the rate of formation of FeC_x. K, present as a carbonate, inhibited oxygen removal but increased the rate of carbon introduction, apparently by increasing CO dissociation rates on FeO_x or FeC_x surfaces.

Mass spectrometric analysis of the products formed during initial exposure of oxide precursors to H_2/CO mixtures at 523 K detected the initial removal of oxygen and a concurrent increase in FTS rates as oxygen was removed and carbon introduced. Steady-state rates were obtained after an initial induction period during which only 1-2 equivalent oxygen monolayers are removed (10^{19} O-atoms/m^2) from the Fe_2O_3 precursors. Pre-reduced (Fe_3O_4) and pre-carburized FeC_x (Fe/C=2.5~3) did not show the induction period or the rapid initial removal of oxygen as H_2O and CO_2 observed on Fe_2O_3 precursors. FTS remained constant even as slow removal of oxygen and introduction of carbon continued to occur on Fe_3O_4. This indicates that the formation of an

active surface occurs within a few FTS turnovers, irrespective of the initial presence of Fe_3O_4 or FeC_x (Fe/C=2.5~3). The catalytic properties of the resulting surface are not influenced by the remaining presence of an oxide or carbide bulk. This active surface is likely to consist of a steady-state mixture of vacancies, adsorbed CO, and carbon and oxygen atoms formed in CO dissociation steps. Their relative concentrations are rapidly established by FTS elementary steps and depend on the redox properties of the contacting gas phase, the reaction temperature, and the surface concentrations of chemical promoters.

In-situ Fe K-edge X-ray absorption (XAS) studies confirmed the phase transformation from Fe_2O_3 to Fe_3O_4 and then to FeC_x during the initial stages of FTS reactions. Only the incipient conversion of Fe_2O_3 to Fe_3O_4 and Fe_xC was required in order to reach steady-state FTS rates. The extent of carburization increased with time on stream without a detectable increase in FTS reaction rates, confirming that the catalytic properties of Fe carbides are not influenced by a remaining Fe oxide core or by its ultimate carburization. Cu, K and Ru all increased the rate and the extent of carbide formation. The promoting effects of K, Cu, and Ru on FTS reaction rates (described below) appear to correlate with their ability to increase the rate and the extent of reduction and carburization of Fe_2O_3 precursors. Localized Fe_2O_3 surface regions influenced by the presence of Cu, Ru, or K species may provide multiple nucleation sites for reduction and carburization within each Fe_2O_3 precursor crystallite with the eventual formation of smaller oxide and carbide particles from larger Fe_2O_3 precursor particles. This proposal is consistent with the greater extent of carburization obtained when K and Cu (Ru) are present.

The effects of promoters (K, Cu and Ru) on FTS rate and selectivity were determined using a fixed-bed reactor in the 493-543 K temperature range and 5-31.6 atm pressure with a H_2/CO mixture (2/1). Addition of Cu considerably improves FTS activity of the catalyst by decreasing the temperature required for the formation of active Fe_xC structures. At 508 K and 21.4 atm for example, the CO rate doubled with the addition of Cu (Cu/Fe=0.01) to a Fe-Zn-K (Zn/Fe=0.1, K/Fe=0.01) catalyst (1.3 to 2.6 mol/h-mol Fe at 20% CO conversion). Copper also promotes the hydrogen availability on the catalyst surface and hence decreases product molecular weight. Potassium improves both the activity and the selectivity of the FTS by increasing the amount of chemisorbed CO and decreasing the amount of chemisorbed H_2 on Fe-based catalysts. The promotion effect of K, however, is much more pronounced on a Cu-promoted catalyst than on a Cu-free catalyst, suggesting a synergistic effect of Cu and K, in agreement with a previous study [1]. Cu and K also significantly promote CO_2 formation during the FTS reaction. Replacement of the Cu by Ru in the Fe-Zn-K system led to a significant promotion of the FT rate (CO rates being 2.7 and 6.7 mol/h-mol Fe respectively at 20% CO conversion and 508 K) with negligible change in the product selectivities. This effect can be attributed to the better dispersion of the Fe_xC structure in the presence of Ru. Furthermore, an increase in surface area in the case of the Fe-Zn-Cu-K catalyst also markedly increases FT rates (CO rates being 2.7 and 6.8 mol/h-mol Fe respectively at 20% CO conversion and 508 K) due to a corresponding increase in the availability of the active Fe_xC sites.

1. S. Soled, E. Iglesia, S. Miseo, B. A. DeRites and R. A. Fiato, *Topics in Catalysis* 2 (1995) 193.

3. Abstract for the 6th Natural Gas Conversion Symposium (NGCS 2001)

Fischer-Tropsch Synthesis Catalysts Based on Fe oxides Modified by Cu and K: Structure and Site Requirements

Senzi Li[1], George D. Meitzner[2], and Enrique Iglesia[1*]

(1) Department of Chemical Engineering, University of California, Berkeley, 94720
(2) Edge Analytical, Inc., 2126 Alllen Blvd., Middleton, WI 53562
* To whom correspondence should be addressed (*Iglesia@cchem.berkeley.edu*.).

INTRODUCTION

Fe, FeC_x, FeO_y, can coexist when Fe oxides are activated in reactive gases or used in Fishcer-Tropsch synthesis (FTS) reactions (1). The relative abundance of these phases depends on reaction conditions and they can influence catalytic performance. The presence and role of these phases remain controversial (2) and the detection of active sites is usually indirect and carried out under non-reactive conditions. In this study, our research effort was focused on developing methods to determine the density of active sites. The structure, reduction and carburization behaviors, and catalytic properties of Fe-based Fischer-Tropsch synthesis (FTS) catalysts were probed using a combination of kinetic, isotopic switch, and spectroscopic methods on Fe-Zn oxides promoted with Cu and K.

EXPERIMENTAL

Fe-Zn precursors (Zn/Fe=0-0.4) were prepared by co-precipitation of Fe nitrate with ammonium carbonate at a constant pH of 7.0, followed by incipient wetness impregnation of the resulting powders with aqueous solutions of potassium carbonate (K/Fe=0-0.04) and/or copper nitrate (Cu/Fe=0-0.02). The dried material was treated in air at 673 K for 4 h. Detailed descriptions of the preparation procedure were reported elsewhere (3).

A rapid switch transient method with on-line mass spectrometry was developed in order to determine initial reduction and carburization behaviors of Fe oxides as well as FTS rates. 0.2 g samples were pretreated in He (100 cm^3/min) at temperatures up to 573 K. The He stream was switched to a flow of 60 % synthesis gas (H_2/CO=2, 100 cm^3/min) at 523 K. The resulting isothermal transients were monitored as a function of time by on-line mass spectrometry. The H_2 and CO chemisorption measurements were carried out after exposure to synthesis gas (H_2/CO=2, 100 cm^3/min) at 523 K for 1 h. The synthesis gas stream was switched to He at 523 K for additional 1 h before quenching to ambient temperatures. A flow of 40% H_2, or 20% CO or 60% synthesis gas in Ar was passed through the samples for 0.5 h. The chemisorbed species were monitored in a temperature-programmed desorption (TPD) mode. The isotopic switch studies (H_2/CO vs. D_2/CO and H_2/^{12}CO vs. H_2/^{13}CO) were conducted at steady-state FTS conditions (H_2/CO=2, 523 K, 100 cm^3/min).

In situ Fe K-edge X-ray absorption near-edge (XANES) and extended X-ray absorption fine structure (EXAFS) analyses of Fe-K-Cu oxides were carried out during FTS in synthesis gas using an XAS cell of our design (4). An 8 mg sample (diluted to 10 wt% Fe using graphite)

was loaded into the cell and synthesis gas (H_2/CO=2) was used at a gas hourly space velocity of 6000 and 523 K.

RESULTS AND DISCUSSION

Reduction studies of Fe-Zn-K-Cu oxides in H_2 showed that K carbonate slightly inhibited the reduction of Fe oxides while Cu increased reduction rates by providing more effective H_2 dissociation sites than those available on Fe_2O_3. Reduction and carburization studies of Fe-Zn-K-Cu in CO showed that these processes occurred in three sequential steps: Fe_2O_3 reduction to Fe_3O_4, Fe_3O_4 reduction to Fe, and ultimate Fe carburization to form χ-$Fe_{2.5}C$ or θ-Fe_3C. Cu decreased the temperature required for Fe_2O_3 reduction and subsequent carburization to Fe carbides. K carbonates increased carburization rates by increasing the rate of CO dissociation on Fe and FeO_x sites.

Mass spectrometric analysis of initial FTS products formed on promoted Fe oxides was used to measure the rate of initial reduction and carburization of Fe_2O_3 precursors and the concomitant increase in FTS rates as oxygen was removed and carbon was introduced during initial activation at 523 K. Steady-state rates were obtained after removal of only about a few layers of the O-atoms in Fe_2O_3, suggesting that only near-surface carbide layers are required to form FTS active sites. The initial product transients on Fe_3O_4 and Fe carbides at FTS conditions showed that instant steady state reaction rates were reached immediately upon contact with H_2/CO mixtures at 523 K on both Fe_3O_4 and Fe carbides; FTS rates remained constant even as Fe_3O_4 continued to reduce and carburize. This indicates that Fe_3O_4 is converted to Fe carbides and that Fe carbides or Fe oxycarbides provide the active surface sites for FTS reactions. Cu increased FTS rates because its presence decreased the temperature required for the formation of active Fe carbide, which may lead to more active carbides with different structures or higher surface areas. The addition of K to Fe-Cu oxides significantly increased not only the reduction and carburization rates and also FTS reaction rates because of higher CO dissociation rates on K-promoted Fe sites.

In-situ Fe K-edge X-ray absorption studies confirmed the phase transformation from Fe_2O_3 to Fe_3O_4 and then to Fe carbides. It was also found that only the incipient conversion of Fe_2O_3 to Fe_3O_4 and Fe_xC was required in order to reach steady-state FTS reaction rates. The extent of carburization increased with time on stream without a detectable increase in FTS reaction rates. This indicates that the surface phase reached the steady state composition required for the FTS reaction. The catalytic properties of Fe carbides appeared not to be influenced by a remaining Fe oxide core or by its ultimate carburization. Cu and K increased carbide formation rates and the proper combination of K-Cu led to stronger effects on the reduction and carburization rates than expected from the individual effects of each component.

H_2 and CO chemisorption on Fe oxides showed that H_2 and CO competitively adsorb on Fe sites. CO occupied two Fe sites while CO was the only adsorbent. In the presence of H_2, a fraction of CO adsorbed molecularly on Fe sites. The addition of K and Cu to Fe_2O_3 significantly increased the site density for H_2 and CO chemisorption. The isotopic exchanges (H_2/CO vs. D_2/CO and $H_2/^{12}CO$ vs. $H_2/^{13}CO$) studies that probed the kinetics of hydrogen dissociation and CO chemisorption and dissociation on a catalyst surface at FTS conditions was also investigated in order to obtain information about the number and reactivity of reaction intermediates.

REFERENCES

(1) Dry, M. E., In Catalysis-Science and Technology; Anderson J. R., and Boudart M. Eds.; Springer Verlag: New York, 1, 196 (1981).

(2) Anderson, R. B., In Catalysis; Emmett, P. H. Eds.; Van Nostrand-Reinhold: New York, 4, 29 (1956).

(3) Soled, S. L., Iglesia, E., Miseo S., DeRites, B, A., Fiato, R. A., Topics in Catalysis, 2, 193 (1995).

(4) Barton, D. G., Ph. D dissertation, University of California, Berkeley, 1998.
(XAS cell developed by Barton, D. G., Biscardi, J. A., and Meitzner, G. D.)

Task 12. Reporting/Project Management

Three monthly and one quarterly reports have been completed.